RSC Medicinal Chemistry

REVIEW

Cite this: *RSC Med. Chem.*, 2023, **14**, 2535

Research status of indole-modified natural products

Song-Fang Duan,†[a] Lei Song,†[b] Hong-Yan Guo,[a] Hao Deng,[a] Xing Huang,[a] Qing-Kun Shen,[a] Zhe-Shan Quan *[a] and Xiu-Mei Yin*[a]

Received 6th October 2023,
Accepted 16th October 2023

DOI: 10.1039/d3md00560g

rsc.li/medchem

Indole is a heterocyclic compound formed by the fusion of a benzene ring and pyrrole ring, which has rich biological activity. Many indole-containing compounds have been sold on the market due to their excellent pharmacological activity. For example, vincristine and reserpine have been widely used in clinical practice. The diverse structures and biological activities of natural products provide abundant resources for the development of new drugs. Therefore, this review classifies natural products by structure, and summarizes the research progress of indole-containing natural product derivatives, their biological activities, structure–activity relationship and research mechanism which has been studied in the past 13 years, so as to provide a basis for the development of new drug development.

1. Introduction

Heterocyclic structures are present in many agents owing to their versatility and biodiversity.[1] Among them, the indole ring is one of the most prevalent heterocycles occurring naturally and in synthetic bioactive compounds.[2,3] Indole is a compound of pyrrole and benzene in parallel, also known as benzopyrrole, and its chemical formula is C_8H_7N. The lone pair of electrons of the nitrogen atom in the indole ring can form a conjugated system with the surrounding π electrons, which enhances the stability and reactivity of the molecule. Therefore, indole is widely used in organic synthesis and drug research.[4] In addition, the N–H group in the indole ring can also form hydrogen bonds with biological macromolecules such as proteins and nucleic acids, thereby affecting biological activity.[5] It is widely distributed in plants such as *Isatidis radix*,[6] *Euodia rutaecarpa*,[7] *Rauvolfia serpentina*,[8] and *Catharanthus roseus*.[9] Indole derivatives have a variety of pharmacological activities,[10] including anti-tumor,[11,12] anti-inflammatory,[13–15] anti-oxidant,[14–17] anti-Alzheimer's,[18] and anti-diabetic[19] activities; therefore, the indole ring plays an important role in the development of new agents. In addition, there are many agents containing indole structures, such as osimertinib, vincristine (VCR), reserpine, tadalafil, fluvastatin, indomethacin, zafirlukast and delavirdine which have been used in clinical research (Fig. 1, Table 1).

Natural products have been used to treat various diseases for thousands of years. In 1578, a large number of cases of using plants to treat human diseases were recorded in the *Compendium of Materia Medica*. For example, the fruit of *Eriobotrya japonica* was used to relieve cough, *Lonicera japonica* was used to cure fever, and so on. Therefore, medicinal natural products are the basis of many early medicines. Natural products extracted and isolated from living organisms play an important role in the discovery and development of new agents and are also important sources of drug candidates.[2] Natural products have great potential for the research and development of new drugs owing to their biodiversity and structural diversity. The use of natural products as lead compounds, combined with structure–bioactivity relationships and metabolic studies for further structural modification and synthesis of derivatives, has become a hot topic in the design and development of new drugs, which often possess higher safety, more efficacy, and cheaper preclinical evaluation.[20] Many natural products are used in their natural form as lead compounds for the treatment of various diseases. Various natural products and their derivatives being used in clinical application include paclitaxel, VCR, morphine, indirubin, codeine, penicillin, *etc.*[21] An increasing number of indole-natural product derivatives are being studied, based on the indole ring exhibiting significant biological activity in pharmaceuticals, which shows the importance of this field.[22–24] Therefore, this paper summarises the research reports on indole-natural product derivatives that have been synthesized in the past 13 years. This review focuses on three aspects *i.e.* biological

[a] *Key Laboratory of Natural Medicines of the Changbai Mountain, Ministry of Education, College of Pharmacy, Interdisciplinary Program of Biological Functional Molecules, College of Integration Science, Yanbian University, Yanji, 133002, China. E-mail: zsquan@ybu.edu.cn, yinxm@ybu.edu.cn; Tel: +86 0433 243 6020, +86 0433 243 6019*

[b] *Yanbian University Hospital, Yanbian University, Yanji 133002, People's Republic of China*

† Song-Fang Duan and Lei Song contributed equally to this work.

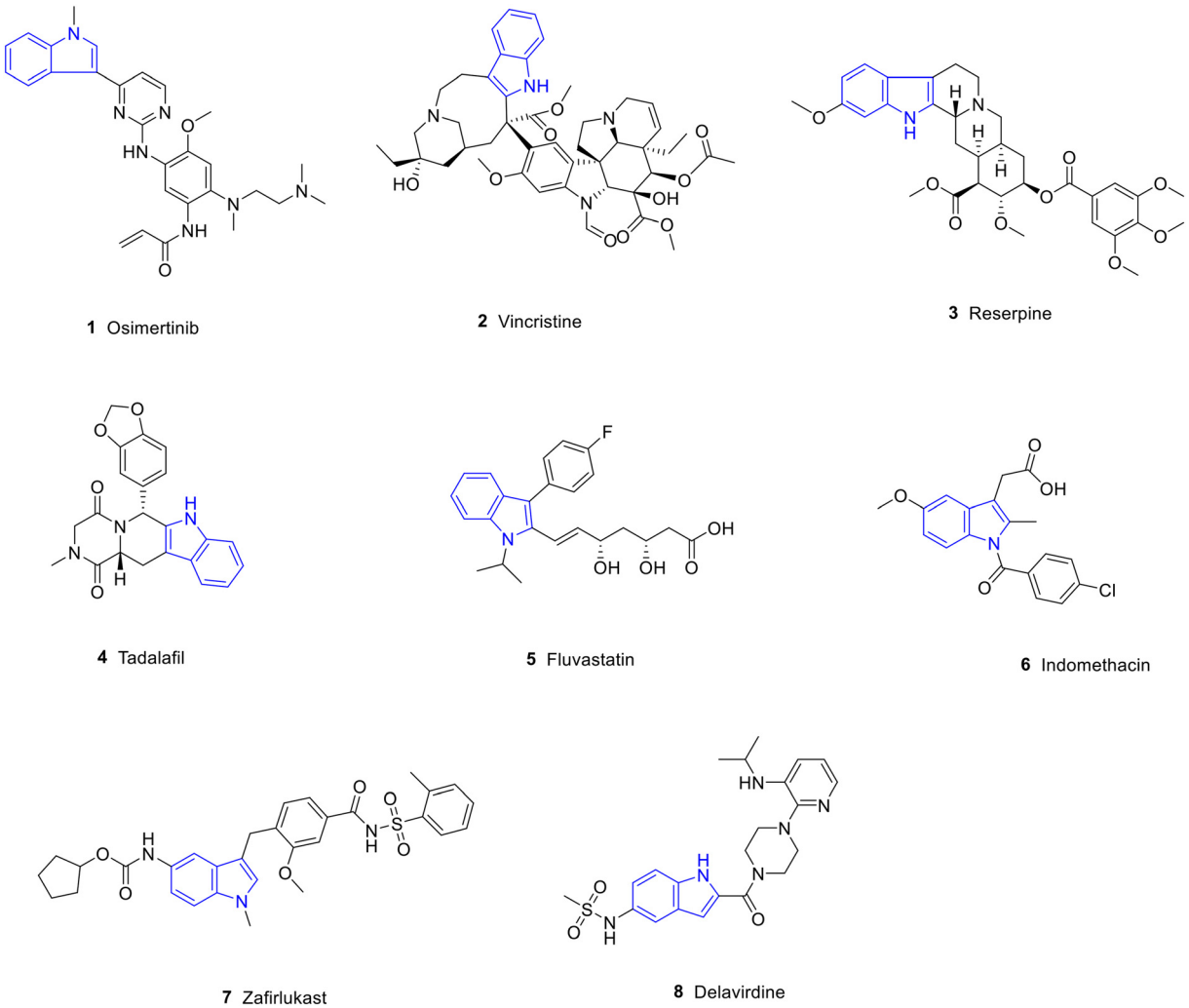

Fig. 1 FDA-approved drugs containing indole structures.

activity, structure–activity relationship, and mechanism of action of promising leads.

2. Methods

In this paper, the keywords "indole", "terpene-indole", "phenylpropanoid-indole", "flavonoid-indole", "alkaloid-indole", "steroid-indole", "polyphenol-indole", "quinone-indole", "structural modification", "pharmacological properties", *etc.* were extensively investigated in the databases such as Pubmed, Web of Science and SciFinder. The research progress of indole-containing natural product derivatives from 2011 to 2023 was summarized in three aspects: structural modification, pharmacological activities and structure–activity relationships.

3. Terpene-indole derivatives

Terpenoids and their derivatives are compounds derived from mevalonate and have isoprene units (C5 units) as the

Table 1 FDA-approved drugs containing indole structures

Compd.	Names	Activity	Targets or mechanisms
1	Osimertinib	Anti-tumor	Mutant-selective EGFR inhibitor
2	VCR	Anti-tumor	Tubulin inhibitor
3	Reserpine	Anti-hypertensive	Blocking the transmission of sympathetic impulses
4	Tadalafil	Anti-pulmonary hypertension	Phosphodiesterase inhibitor
5	Fluvastatin	Hypolipidemic	Inhibition of endogenous cholesterol synthesis
6	Indomethacin	Anti-inflammatory	Cyclooxygenase inhibitor
7	Zafirlukast	Anti-asthma	Leukotriene receptor antagonist
8	Delavirdine	Anti-HIV	Reverse transcriptase inhibitor

basic structural unit of the molecular backbone.[25] Terpenoids are structurally complex and can be classified into eight groups according to the number of isoprene units: hemiterpenoids, monoterpenes, sesquiterpenes, diterpenes, sesterterpenoids, triterpenes, tetraterpenes, and polyterpenoids. Terpenoids are widely found in nature, with a wide variety of species and skeletons, and they are the most abundant compounds in natural products.[26] More than 60 000 terpenoids have been discovered to date, and these compounds have a variety of biological activities, including anti-tumor,[27] anti-oxidant,[28] anti-bacterial,[29] hypolipidaemic[30] and other pharmacological activities.

Genipin is a natural product of iridoids, obtained by the hydrolysis of gardenia glycosides by β-glucosidase, with pharmacological activities such as anti-tumor activity.[31] Fang *et al.* synthesized 34 genipin-indole derivatives and determined their cytotoxic activities against SW480, A-549, HL60, SMMC-7721 and MCF-7 cancer cells. Derivatives **9** (Fig. 2, Table 2, IC_{50}: 0.9–3.64 μM) and **10** (Fig. 2, Table 2, IC_{50}: 0.43–1.18 μM) showed strong anti-proliferative activity against SW480, A549, HL60, SMMC-7721 and MCF-7 cancer cells, with inhibition rates above 98%. Further experiments showed that compound **10** induced apoptosis and arrested the cell cycle.[32]

Parthenolide is a natural product of sesquiterpene lactones, which is derived from the flower buds of *Tanacetum balsamita* and possesses anti-tumor activity.[33] Bommagani *et al.* designed and synthesized a series of parthenolide-indole derivatives, hoping to obtain promising drugs against hematological tumors. Derivative **11** (Fig. 2, Table 2, GI_{50}: 0.26–0.28 μM) showed considerable growth inhibitory activity against RPMI-8226 and CCRF-CEM cancer cell lines and was 32 fold more potent than parthenolide (GI_{50}: 8.20–9.16 μM). Further modification showed that the introduction of a methoxy group as well as halogen groups such as fluorine and chlorine on the benzene ring was not conducive to anti-proliferative activity. Indole-3-carboxylate (compound **12**) (Fig. 2, Table 2, GI_{50}: 0.04–0.05 μM) displayed much lower growth inhibitory activity on RPMI-8226 and CCRF-CEM, suggesting that the connection to the indole C-3 position can improve the cells of the compound toxicity. Furthermore, the introduction of Michael receptors is beneficial for anti-proliferative activity. Compound **13** (Fig. 2, Table 2, GI_{50}: 0.03–0.07 μM), obtained by replacing the carboxylic acid group with acrylic acid, exhibited stronger anti-proliferative activity. The results of the M9-ENL1 AML cell assay showed that compound **13** (EC_{50}: 0.72 μM) exhibited the highest anti-proliferative activity against M9-ENL1 AML cancer cells and was 20 fold more potent than parthenolide (EC_{50}: 15 μM).[34]

Artemisinin is a natural product of sesquiterpene lactones, which is derived from the stems and leaves of *Artemisia carvifolia* and possesses anti-tumor[35] and anti-*Toxoplasma*

Table 2 Biological activity of monoterpenoid-indole derivatives **9**–**10** and sesquiterpenoid-indole derivatives **11**–**16**

Compd.	Activity	Ref.
9	HL-60 cells: IC_{50} = 0.9 μM A549 cells: IC_{50} = 3.64 μM SMMC-7721 cells: IC_{50} = 3.52 μM MCF-7 cells: IC_{50} = 3.10 μM SW480 cells: IC_{50} = 2.53 μM	21
10	HL-60 cells: IC_{50} = 0.43 μM A549 cells: IC_{50} = 1.18 μM SMMC-7721 cells: IC_{50} = 0.69 μM MCF-7 cells: IC_{50} = 0.58 μM SW480 cells: IC_{50} = 0.89 μM	21
11	RPMI-8226 cells: GI_{50} = 0.26 μM CCRF-CEM cells: GI_{50} = 0.28 μM	23
12	RPMI-8226 cells: GI_{50} = 0.04 μM CCRF-CEM cells: GI_{50} = 0.05 μM	23
13	RPMI-8226 cells: GI_{50} = 0.03 μM CCRF-CEM cells: GI_{50} = 0.07 μM M9-ENL1 AML cells: EC_{50} = 0.72 μM	23
Parthenolide	RPMI-8226 cells: GI_{50} = 8.20 μM CCRF-CEM cells: GI_{50} = 9.16 μM M9-ENL1 AML cells: EC_{50} = 15 μM	23
14	MCF-7 cells: IC_{50} = 5.25 μM A549 cells: IC_{50} = 6.17 μM *T. gondii*-infected HeLa cells: IC_{50} = 85.3 μM	14, 26
15	MCF-7 cells: IC_{50} = 14.48 μM A549 cells: IC_{50} = 13.39 μM	26
16	MCF-7 cells: IC_{50} = 6.78 μM A549 cells: IC_{50} = 12.92 μM	26

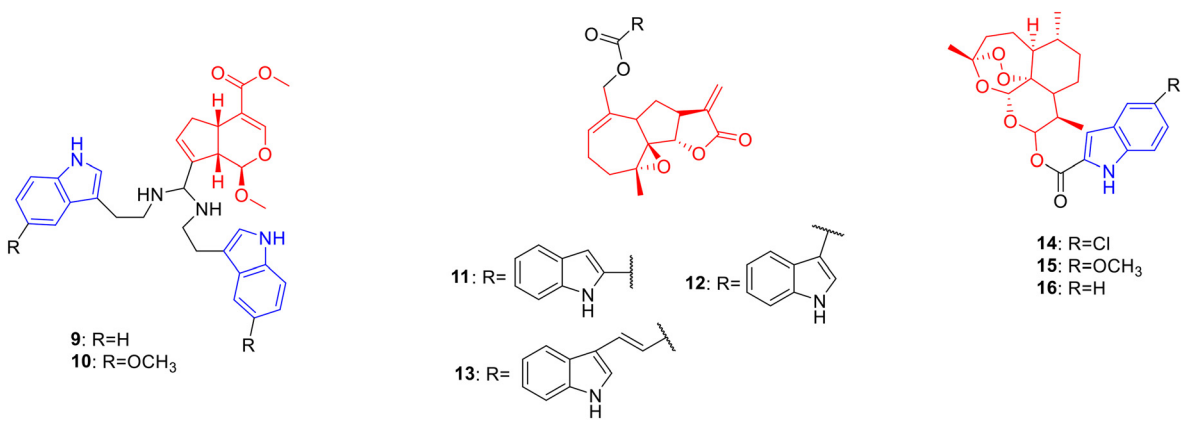

Fig. 2 Chemical structures of monoterpenoid-indole derivatives **9**–**10** and sesquiterpenoid-indole derivatives **11**–**16**.

gondii activities.[36] Hu *et al.* designed and synthesized a series of artemisinin-indole derivatives and evaluated their cytotoxic activities against A549, MCF-7, HepG-2 and MDA-MB-231 cancer cells. Derivatives **14** (Fig. 2, Table 2, IC_{50}: 5.25–6.17 μM), **15** (Fig. 2, Table 2, IC_{50}: 13.39–14.48 μM) and **16** (Fig. 2, Table 2, IC_{50}: 6.78–12.92 μM) showed high activity against MCF-7 and A549 cancer cell lines. Compound **14** with an electron-withdrawing group was generally more potent than compounds **15** and **16** against MCF-7 and A549 cells, indicating that the electron-withdrawing group on the benzene ring contributed more to the anti-proliferative activity. Further studies illustrated that compound **14** (reversal fold (RF): 117) could reverse the multidrug resistance of MCF-7/doxorubicin cells and induce G2/M cell cycle arrest in MCF-7 cells. Therefore, compound **14** can serve as a potential anticancer drug for reversing multidrug resistance and is worthy of further study.[37] In addition, Deng's study showed that compound **14** exhibited promising anti-*T. gondii* activity with a selectivity of 1.58 and IC_{50} value of 85.3 in *T. gondii*-infected HeLa cells, being more potent than spiramycin with a selectivity of 0.72 and IC_{50} value of 262.2 in *T. gondii*-infected HeLa cells.[23]

Retinoic acid is a monocyclic diterpene natural product metabolised from vitamin A, which possesses anti-tumor activity.[38] Gurkan-Alp *et al.* designed and synthesized five retinoic acid-indole derivatives and determined their anti-tumor activity *in vitro*. Derivative **17** (Fig. 3, Table 3, IC_{50}: <0.01–1.83 μM) exhibited low-concentration anti-proliferative activity against Cama1, MCF-7, MDA-MB-453, SK-BR-3, MDA-MB-361 and MDA-MB-231 breast cancer cell lines as well as being comparable to camptothecin (IC_{50}: <0.01–0.17 μM). In addition, compound **17** showed the strongest anti-proliferative activity against Cama1 and MDA-MB-453 (IC_{50} values below 0.01 μM), while the less toxic effect on normal epithelial breast cancer cell line MCF-12A was relatively small with an IC_{50} value of 3.92 μM. Interestingly, compound **17** displayed potent anti-proliferative activity against MDA-MB-231, a triple-negative breast cancer cell line, with an IC_{50} value of 1.83 μM. Further studies indicated that compound **17** induced apoptosis in MDA-MB-231 cells, which may be related to the inhibition of the RXRa receptors. Therefore, compound **17** can be used as a candidate agent for the treatment of triple-negative breast cancer, and is worthy of further study.[39]

Table 3 Biological activity of diterpenoid-indole derivatives **17–22**

Compd.	Activity	Ref.
17	Cama1 cells: IC_{50} < 0.01 μM MCF-7 cells: IC_{50} = 1.71 μM MDA-MB-453 cells: IC_{50} < 0.01 μM SK-BR-3 cells: IC_{50} = 1.29 μM MDA-MB-361 cells: IC_{50} = 0.06 μM MDA-MB-231 cells: IC_{50} = 1.83 μM MCF-12A cells: IC_{50} = 3.92 μM	28
Camptothecin	Cama1 cells: IC_{50} = 0.07 μM MCF-7 cells: IC_{50} < 0.01 μM MDA-MB-453 cells: IC_{50} < 0.01 μM SK-BR-3 cells: IC_{50} < 0.01 μM MDA-MB-361 cells: IC_{50} = 0.17 μM MDA-MB-231 cells: IC_{50} < 0.01 μM	28
18	MCF-7 cells: IC_{50} = 1.85 μM HCT116 cells: IC_{50} = 1.22 μM	30
19	SMMC-7721 cells: IC_{50} < 1.39 μM HepG2 cells: IC_{50} = 0.51 μM Hep3B cells: IC_{50} < 0.73 μM	32
20	HCT116 cells: IC_{50} = 0.81 μM Bel7402 cells: IC_{50} = 0.83 μM MCF-7 cells: IC_{50} = 0.39 μM	15
21	HCT116 cells: IC_{50} = 0.68 μM Bel7402 cells: IC_{50} = 1.73 μM MCF-7 cells: IC_{50} = 0.83 μM	15
22	HCT116 cells: IC_{50} = 0.16 μM Bel7402 cells: IC_{50} = 2.18 μM MCF-7 cells: IC_{50} = 1.52 μM	15
Oridonin	HCT116 cells: IC_{50} = 6.84 μM	15
5-Fu	HCT116 cells: IC_{50} = 24.8 μM	15

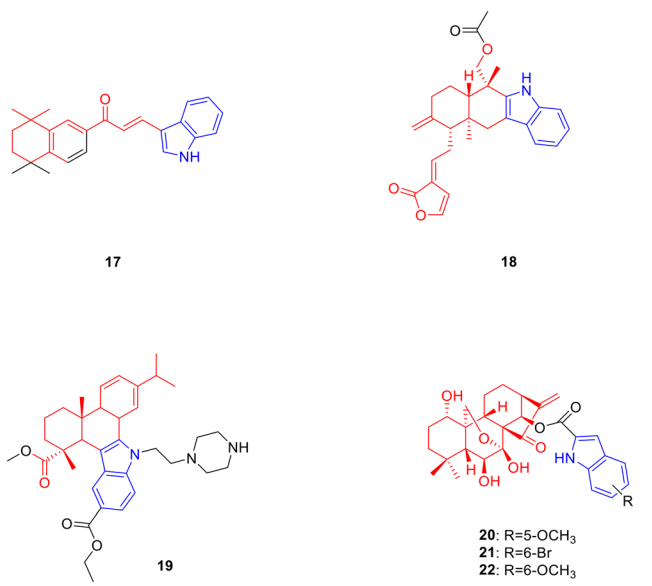

Fig. 3 Chemical structures of diterpenoid-indole derivatives **17–22**.

Andrographolide is a bicyclic diterpene lactone natural product derived from *Andrographis paniculata* that possesses anti-tumor activity.[40,41] Song *et al.* synthesized a series of novel indolo [3,2-*b*] andrographolide derivatives and determined their cytotoxic activities against three human cancer cell lines MCF7, HCT116 and DU145. Derivative **18** (Fig. 3, Table 3, IC_{50}: 1.22–1.85 μM) showed considerable anti-proliferative activity against MCF-7 and HCT116 cancer cell lines. SAR analysis indicated that the anti-proliferative activity of the bisesterified compounds of the C-14 and C-19 hydroxyl groups was stronger than that of the monoesterified compounds, and the steric hindrance of the ester group also affected the anti-proliferative activity of the compounds. A smaller volume of acetyl groups exhibited stronger anti-proliferative activity than benzoyl groups. Further experiments showed that compound **18** induced HCT116 cell arrest in the S phase and induced apoptosis in a concentration-dependent manner.[42]

Dehydroabietic acid is a tricyclic diterpenoid oxygenated compound, which is widely present in all types of Pinaceae plants and exhibits antitumour activity.[43] Chen *et al.* designed and synthesized a series of novel dehydroabietic acid-indole derivatives, and evaluated their anticancer activities against SMMC-7721, HepG2 and Hep3B cancer cells. Derivative **19** (Fig. 3, Table 3, IC_{50}: 0.51–1.39 μM) showed strong cytotoxic activities against SMMC-7721, HepG2 and Hep3B cancer cell lines. Mechanistic studies indicated that compound **19** inhibited the MAPK signalling pathway, increased ROS generation, arrested the cell cycle in the G2/M phase, and damaged membrane integrity. Overall, compound **19** is a promising anticancer agent candidate.[44]

Oridonin is a tetracyclic diterpene natural product derived from the whole plant of *Isodon rubescens* with anti-tumor activity.[45] Shen *et al.* designed and synthesized a series of oridonin derivatives, and found that when bearing an indole ring on the 14-OH position, the oridonin derivatives had the best anti-tumour activity. Derivatives **20** (Fig. 3, Table 3, IC_{50}: 0.39–0.83 μM), **21** (Fig. 3, Table 3, IC_{50}: 0.68–1.73 μM) and **22** (Fig. 3, Table 3, IC_{50}: 0.16–2.18 μM) exhibited considerable activities against HCT116, Bel7402 and MCF-7 cancer cells. In particular, compound **22** showed extremely potent anti-proliferative activity against HCT116 cancer cells with an IC_{50} value of 0.16 μM, and was 43 times higher than oridonin (IC_{50}: 6.84 μM) as well as 155 times the positive control drug 5-fluorouracil (5-Fu) (IC_{50}: 24.8 μM). The selectivity of compound **22** for HCT116 cells (selection coefficient: 23.63) was stronger than that for normal L02 cells, and the selection effect was better than that of oridonin (selection coefficient: 1.02) and 5-Fu (selection coefficient: 0.65). SAR analysis showed that the properties and positions of the substituents on the indole ring were closely related to the anti-proliferative activity of the compounds, and the activity sequence was: 6-OCH_3 > 6-F > 6-Br > 5-OCH_3 > 6-Cl> 5-Cl > 5-H. Furthermore, compound **22** inhibited colony formation by HCT116 cells in a concentration-dependent manner. Further experiments revealed that compound **22** may induce G2/M phase arrest and apoptosis in HCT116 cells *via* the p53-MDM2 pathway. *In vivo* experiments showed that compared with the control group, the tumour volume and weight after compound **22** treatment were significantly decreased. Overall, compound **22** is a highly potential anti-tumor drug that deserves further study.[24]

Malabaricol is a tricyclic triterpenoid natural product derived from the gum exudates of the trunk of *Ailanthus*

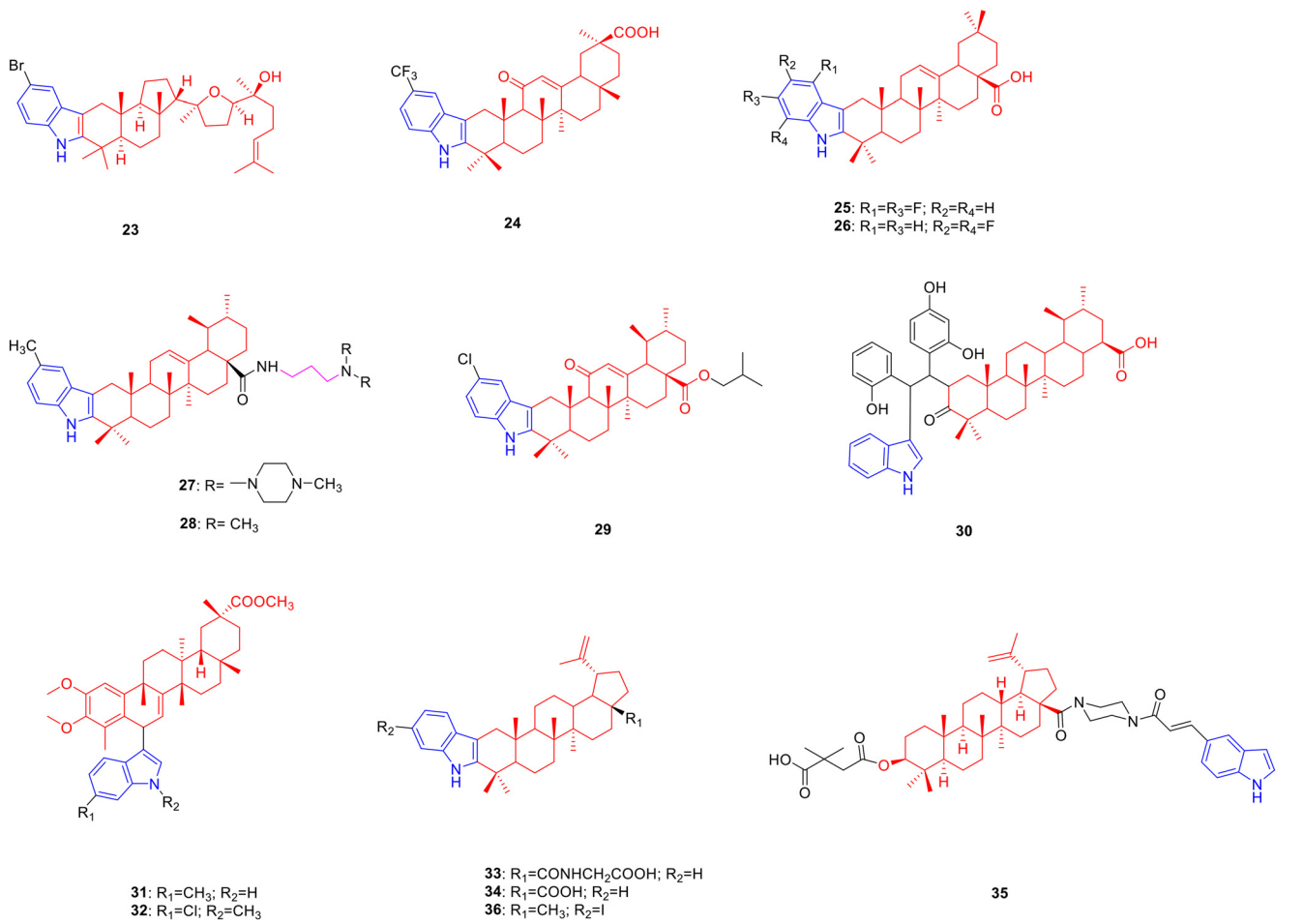

Fig. 4 Chemical structures of triterpenoid-indole derivatives **23**–**36**.

triphysa and exhibits anti-tumour activity.[46] Bommakanti *et al.* synthesized a series of malabaricol derivatives and determined their cytotoxic activity against A549 cancer cells. Derivative **23** (Fig. 4, Table 4, IC_{50}: 13.40 μM) showed promising activity against A549 cancer cells, being comparable to malabaricol (IC_{50}: 10.91 μM).[22]

Glycyrrhetinic acid is a natural product of pentacyclic triterpenes, which is derived from the root of *Glycyrrhiza uralensis* and possesses hypoglycaemic activity.[47] De-la-Cruz-Martínez *et al.* designed and synthesized a series of glycyrrhetinic acid derivatives, expecting to obtain potential new hypoglycemic drugs. Derivative **24** (Fig. 4, Table 4, IC_{50}: 4.3 μM) showed considerable inhibitory activity against PTP1B. The SAR illustrated that the introduction of trifluoromethyl, methoxy, and fluorine atoms enhanced the inhibitory activity, whereas the introduction of methyl and chlorine atoms reduced the activity. Enzyme kinetics experiments showed that compound **24** (Ki: 3.9 μM) is a non-competitive inhibitor with stronger binding ability to the enzyme than suramin (Ki: 7.1 μM).[48]

Oleanolic acid is a pentacyclic triterpenoid natural product derived from the fruit of *Ligustrum lucidum* and has pharmacological activities such as inhibition of glucosidase,[49] anti-oxidant,[50] and anti-hyaluronidase.[50] Therefore, researchers modified the C2 and C3 positions of oleanolic acid to obtain compounds with better pharmacological activity. Derivative **25** (Fig. 4, Table 4, IC_{50}:4.02 μM) showed considerable inhibitory activity against α-glucosidase. The SAR results showed that the introduction of an indole group at the C-3 position of oleanolic acid could enhance the biological activity of the compound, the carboxyl group at the C-28 position was crucial to the activity of the compound, and esterification of the carboxyl group greatly reduced its activity. The results of enzyme kinetics analysis revealed that compound **25** is a mixed type of α-glucosidase inhibitor, and the mechanism of action is to inhibit the formation of the α-glucosidase-*p*-NPG intermediate by binding to α-glucosidase and to the substrate *p*-NPG of α-glucosidase directly.[51]

Derivative **26** (Fig. 4, Table 4, IC_{50}: 9.97 μM) exhibited high inhibitory activity against hyaluronidase. Compared to heterocycles such as quinoline and pyridine, the introduction of an indole ring can improve the biological activity of the compound. Further studies illustrated that compound **26** was a mixed non-competitive enzyme inhibitor, which reduced enzyme activity by binding to the aromatic amino acid side chain of the hyaluronidase protein. Moreover, compound **26** exhibited skin permeability under weakly acidic conditions (pH = 6.5). *In vitro* studies showed that, compared with oleanolic acid, compound **26** significantly reduced ROS levels in HaCAT cells and ameliorated H_2O_2-induced oxidative stress. Overall, compound **26** is a potential agent with anti-hyaluronidase activity, which has further research value.[52]

Ursolic acid is a pentacyclic triterpenoid natural product derived from the fruit of *Arctostaphylos uva-ursi* with anti-tumor activity.[53] Therefore, researchers have modified the C2, C3 positions and carboxyl group of ursolic acid, hoping to obtain anti-tumor drugs with research prospects. Derivatives **27** (Fig. 4, Table 4, IC_{50}: 0.56–0.91 μM)[54] and **28** (Fig. 4, Table 4, IC_{50}: 1.08–1.26 μM)[55] showed strong inhibitory activity against SMMC-7721 and HepG2. Among them, compound **28** was comparable to doxorubicin (IC_{50}: 0.62–0.77 μM) and compound **27** was less toxic to human normal hepatocytes L02 with an IC_{50} value of 10.58 μM. SAR analysis of compound **27** indicated that when the number of carbon atoms in the alkyl linker between the amide group and the amino group was three, the best tumour inhibitory effect was exhibited. The type of nitrogen-containing structure in the side chain is also closely related to the anti-proliferative activity of the compound. The introduction of methylpiperazine, $-NH_2$, $-N(Me)_2$, $-N(Et)_2$, and piperidine increased the anti-proliferative activity of the compounds. Among them, the effect of *N*-methylpiperazine was the most obvious, whereas the anti-proliferative activity of compounds containing morpholine structures was not obvious. The SAR analysis of compound **28** indicated that the introduction of a substituent at the C-5 position of the indole ring could enhance anti-tumor activity, while the introduction of a substituent at the C-7 position greatly reduced anti-proliferative activity.

Further studies showed that compound **27** not only inhibited the relaxation of supercoiled DNA by inhibiting the activity of topoisomerase II but also induced the production of ROS and decreased membrane potential in SMMC-7721 cells in a dose-dependent manner to induce apoptosis. Compound **27** had a significant topoisomerase II inhibitory

Table 4 Biological activity of triterpenoid-indole derivatives **23–36**

Compd.	Activity	Ref.
23	A549 cells: IC_{50} = 13.40 μM	13
24	Protein tyrosine phosphatase 1 B: IC_{50} = 4.3 μM	36
25	α-Glucosidase: IC_{50} = 4.02 μM	39
26	Hyaluronidase: IC_{50} = 9.97 μM	40
27	SMMC-7721 cells: IC_{50} = 0.56 μM HepG2 cells: IC_{50} = 0.91 μM	42
28	SMMC-7721 cells: IC_{50} = 1.08 μM HepG2 cells: IC_{50} = 1.26 μM	45
29	HepG2 cells: IC_{50} = 3.12 μM SGC7901 cells: IC_{50} = 10.22 μM	44
Paclitaxel	HepG2 cells: IC_{50} = 7.87 μM SGC7901 cells: IC_{50} = 14.35 μM	44
Ursolic acid	HepG2 cells: $IC_{50} > 20$ μM SGC7901 cells: $IC_{50} > 20$ μM	44
31	Bel7402 cells: IC_{50} = 0.02 μM	47
32	H4 cells: IC_{50} = 2.03 μM Bel7402 cells: IC_{50} = 0.01 μM	47
Celastrol	H4 cells: IC_{50} = 2.09 μM Bel7402 cells: IC_{50} = 1.55 μM	47
33	α-Glucosidase: IC_{50} = 1.8 μM	50
34	α-Glucosidase: IC_{50} = 0.04 μM	51
Acarbose	α-Glucosidase: IC_{50} = 189.2 μM	51
35	HIV-1 cells: IC_{50} = 0.05 μM	52
Bevirimat	HIV-1 cells: IC_{50} = 0.065 μM	52
36	RAW 264.7 cells: IC_{50} = 22.6 μM	54
Lupeol	RAW 264.7 cells: IC_{50} = 37.3 μM	54

effect, strong anti-cancer activity, and selectivity, and can be used as an anti-cancer drug for further research.

Derivative **29** (Fig. 4, Table 4, IC_{50}: 3.12–10.22 μM) exhibited promising activity against HepG2 and SGC7901 cancer cells, being more potent than ursolic acid (IC_{50}: >20 μM) and paclitaxel (IC_{50}: 7.87–14.35 μM). In addition, at a concentration of 10 μM, compound **29** (48.96% and 54.6% inhibition, respectively) inhibited the growth of HepG2 and SGC7901 cells compared to paclitaxel (52.75% and 50.82% inhibition, respectively), and was superior to ursolic acid (12.62% and 13.34% inhibition, respectively). SAR results showed that haloalkanes with branched chains were more active than straight-chain haloalkanes; meanwhile, the anti-tumor activity of haloalkanes increased with the growth of their carbon chains.[56]

Derivative **30** (Fig. 4) exhibited considerable anti-proliferative activity against U251 and C6 glioma cells (the proliferation rate was reduced to 17% and 21% at 10 μM, respectively). Mechanistic studies revealed that compound **30** could downregulate cAMP levels and induce G0/G1 phase arrest and apoptosis in U251 glioma cells. Therefore, compound **30** could be further studied as a potential anticancer drug.[57]

Celastrol is a pentacyclic triterpenoid natural product derived from the whole plant or peeled xylem of *Tripterygium wilfordii*, possessing anti-tumor activity.[58] Tang *et al.* synthesized a series of C(6)-indole-substituted celastrol derivatives and explored their antitumor activity against Bel7402 cells. Derivatives **31** (Fig. 4, Table 4, IC_{50}: 0.02 μM) and **32** (Fig. 4, Table 4, IC_{50}: 0.01 μM) showed considerable anti-proliferative activity against human hepatocellular carcinoma Bel7402. Although most compounds substituted at the C-5 position of the indole ring are more cytotoxic than those substituted at the C-6 position, the C-6 substituted celastrol-indole derivative **31** is highly cytotoxic to human hepatocellular carcinoma Bel7402 which showed excellent anti-proliferative activity and was 77 fold more potent than celastrol (IC_{50}: 1.55 μM). In addition, the *N*-substituted indole derivative **32** not only showed good anti-proliferative activity against Bel7402 cancer cells but also exhibited similar anti-proliferative activity to celastrol (IC_{50}: 2.09 μM) against the human glioblastoma cell line H4 (IC_{50}: 2.03 μM).[59]

Betulinic acid is a common pentacyclic triterpenoid derived from *Betula platyphylla*, which has hypoglycaemic[60] and antiviral activities.[61] Therefore, researchers have designed and synthesized a series of betulinic acid-indole derivatives, expecting to obtain new drugs with excellent biological activity. The inhibitory activity of derivative **33** (Fig. 4, Table 4, IC_{50}: 1.8 μM) against α-glucosidase being 10 fold more potent active than betulinic acid (IC_{50}: 18.4 μM) illustrated that the C-2 and C-3 positions of betulinic acid fused into the indole ring can significantly increase the activity.[62] Further structural modifications revealed that compound **34** (Fig. 4, Table 4, IC_{50}: 0.04 μM), with the replacement of the carboxyl group at C-28 with a carboxamide group, was 4730 fold more potent active than acarbose (IC_{50}: 189.2 μM), probably because the carboxamide group provided more hydrogen bonds than the carboxyl group.[63] In addition, derivative **35** (Fig. 4, Table 4, IC_{50}: 0.05 μM) exhibited considerable activity against HIV-1, being more potent than bevirimat (IC_{50}: 0.065 μM).[64]

Lupeol is a triterpenoid derived from the cuticle of lupin seeds that exhibits anti-inflammatory pharmacological activity.[65] Bhandari *et al.* synthesized a series of lupeol indole derivatives, expecting to obtain new drugs with excellent anti-inflammatory activity. Lupeol-indole derivative **36** (Fig. 4, Table 4, IC_{50}: 22.6 μM on RAW 264.7 cells) was more active in inhibiting NO production than lupeol (IC_{50}: 37.3 μM on RAW 264.7 cells), and the SAR studies showed that substituted electron donating groups on the indole benzene ring promote the activity. Furthermore, at the concentration of 20 μg mL^{-1}, the TNF-α and IL-1β inhibitory activities of compound **36** on RAW 264.7 cells were 42.3% and 22.9%, respectively, while the inhibitory activities of curcumin on TNF-α and IL-1β were 1.25% and 6.44%, respectively.[66]

Summary: there were many reports on the anti-tumor activity of indole-modified terpenoid natural products. Among them, oridonin-indole derivative **22** show 43 times higher anti-HCT116 cancer cell activity than oridonin, and the IC_{50} value was 0.16 μM. The activity of the substituent at the C6 position was significantly stronger than that of C5, and the electron-donating group improved the activity of the compound. Therefore, compound **22** had further research value.

4. Phenylpropanoid-indole derivatives

Phenylpropanoids are a class of compounds consisting of a benzene ring linked to three straight-chain carbon atoms (C6–C3 groups), including phenylpropylenes and their derivatives with different degrees of oxidation, coumarins, and lignans, which have pharmacological activities such as anti-tumor,[67] anti-bacterial,[68] hypolipidaemic[69] and anti-oxidant.[70]

Podophyllotoxin is an aryl tetrahydronaphtholide lignan natural product, which is derived from the rhizome of *Podophyllum versipelle* and possesses anti-tumor activity.[71] Therefore, researchers modified the C4 position of podophyllotoxin in order to obtain antitumor drugs with research value. Derivative **37** (Fig. 5, Table 5, IC_{50}: 0.07–0.1 μM) showed excellent anti-tumor activity against HepG2, HeLa, A549 and MCF-7 cancer cell lines, and was 26–58 fold more potent than podophyllotoxin (IC_{50}: 2.4–6.9 μM) as well as 24–86 fold more potent than colchicine (IC_{50}: 9.7–14.3 μM), respectively. Further studies illustrated that compound **37** induced G2/M phase arrest and inhibited tubulin polymerisation. *In vivo* experiments showed that compound **29** significantly inhibited tumour growth. Therefore, compound **37** has further research value as a potential tubulin inhibitor.[72]

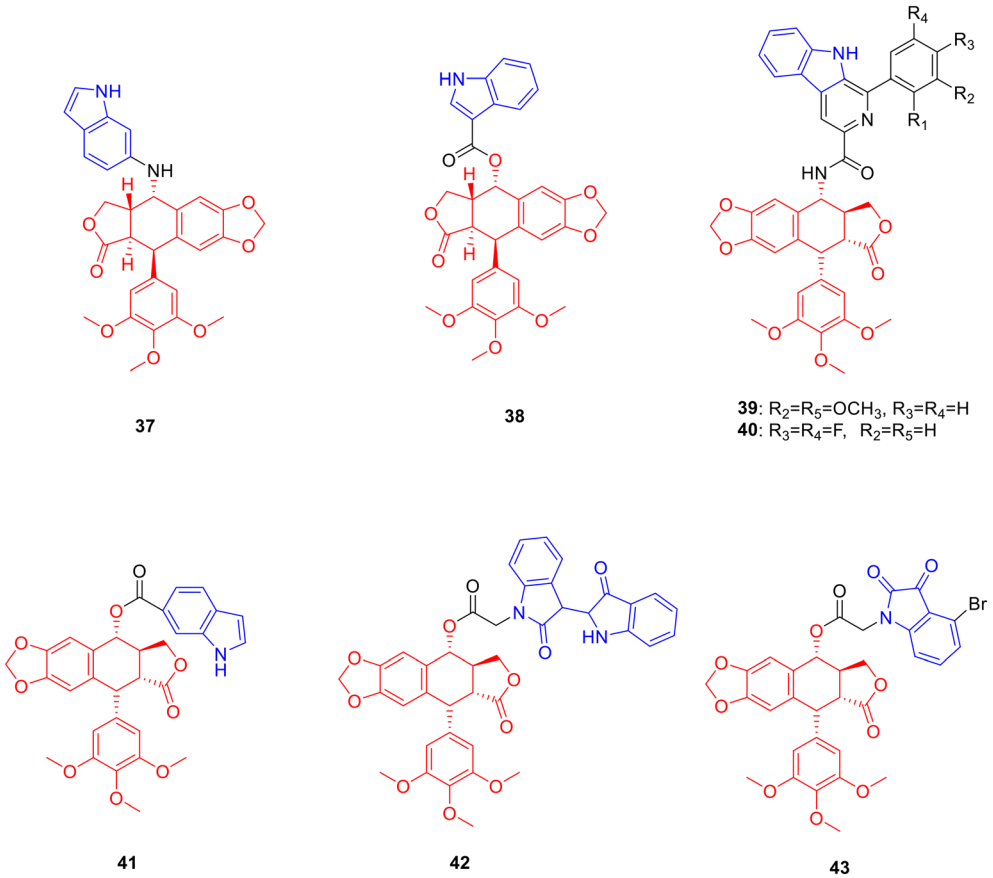

Fig. 5 Chemical structures of podophyllotoxin-indole derivatives **37**–**43**.

The anti-proliferative activity of derivative **38** (Fig. 5, Table 5, IC_{50}: 1.93–2.2 μM) was stronger than podophyllotoxin (IC_{50}: 6.21–9.32 μM) against HepG2 and HeLa cells; it was also less toxic against LO2 cells (IC_{50}: 75.66 μM) and PBMC cells (IC_{50}: 88.97 μM). Further experiments showed that compound **38** induced cell arrest in the G2/M phase and apoptosis through the mediation of Bcl-2.[73]

Table 5 Biological activity of podophyllotoxin-indole derivatives **37**–**42**

Compd.	Activity	Ref.
37	HepG2 cells: IC_{50} = 0. 1 μM HeLa cells: IC_{50} = 0.08 μM A549 cells: IC_{50} = 0.08 μM MCF-7 cells: IC_{50} = 0.07 μM	60
Podophyllotoxin	HepG2 cells: IC_{50} = 2.4 μM HeLa cells: IC_{50} = 6.9 μM A549 cells: IC_{50} = 2.6 μM MCF-7 cells: IC_{50} = 2.4 μM	60
Colchicine	HepG2 cells: IC_{50} = 5.8 μM HeLa cells: IC_{50} = 10.2 μM A549 cells: IC_{50} = 9.7 μM MCF-7 cells: IC_{50} = 14.3 μM	60
38	HepG2 cells: IC_{50} = 1.93 μM HeLa cells: IC_{50} = 2.2 μM	61
Podophyllotoxin	HepG2 cells: IC_{50} = 6.21 μM HeLa cells: IC_{50} = 9.32 μM	61
39	A549 cells: IC_{50} = 1.87 μM	62
40	A549 cells: IC_{50} = 2.24 μM	62
Podophyllotoxin	A549 cells: IC_{50} = 3.76 μM	62
VP-16	A549 cells: IC_{50} = 2.27 μM	62
41	K562 cells: IC_{50} = 0.1 μM	63
42	K562 cells: IC_{50} = 0.034 μM	64
VP-16	K562 cells: IC_{50} = 0.764 μM	64
VCR	K562 cells: IC_{50} = 0.178 μM	64

Derivatives **39** (Fig. 5, Table 5, IC_{50}: 1.87 μM) and **40** (Fig. 5, Table 5, IC_{50}: 2.24 μM) showed strong anti-proliferative activity against A549 cancer cells, being more potent than podophyllotoxin (IC_{50}: 3.76 μM) and etoposide (VP-16) (IC_{50}: 2.27 μM). Further studies illustrated that compounds **39** and **40** induced cell G2/M phase arrest, inhibited topoisomerase II activity, and bound to DNA. Therefore, compounds **39** and **40** deserve further study as potential topoisomerase II inhibitors.[74]

Derivative **41** (Fig. 5, Table 5, IC_{50}: 0.1 μM) showed promising anti-proliferative activity against K562 cancer cells, which was comparable to podophyllotoxin (IC_{50}: 0.025 μM) and VCR (IC_{50}: 0.178 μM). In addition, compound **41** (resistance factor value: 2.27) also displayed a lower resistance factor in K562/VCR cells, which was comparable to podophyllotoxin (resistance factor value: 2.00) but much lower than VP-16 (resistance factor value: 15.497) and VCR (resistance factor value: 26.612).[75] Derivative **42** (Fig. 5, Table 5, IC_{50}: 0.034 μM; the resistance factor values of compound **42**, podophyllotoxin, VP-16, and VCR were 2.23, 2.00, 15.49, and 26.61, respectively) showed a lower

resistance factor against K562/VCR, and exhibited promising anti-proliferative activity against K562 cancer cells, being more potent than VP-16 (IC_{50}: 0.764 μM) and VCR (IC_{50}: 0.178 μM), and comparable to podophyllotoxin (IC_{50}: 0.025 μM).[76] In addition, compound **41** induced autophagy in K562/VCR cells by inhibiting the PI3K/AKT/mTOR signalling pathway, while compound **42** induced autophagy in K562/VCR cells by increasing the levels of Beclin1 and LC3-II.

Derivative **43** (Fig. 5) (resistance factor value: 3.5) showed lower resistance against K562/ADR cancer cells than podophyllotoxin (resistance factor value: 14.166) and VP-16 (resistance factor value: 4.903). Preliminary experiments showed that compound **43** disrupted the tubulin structure, induced cell G2 arrest and apoptosis, and reversed the drug resistance of tumour cells by downregulating the expression levels of P-gp and MRP1 proteins.[77]

Derivative **44** (Fig. 6, Table 6, IC_{50}: 5.87 μM) showed considerable anti-proliferative activity against Bel-7402 cancer cells, which was comparable to that of 5-Fu (IC_{50}: 5.94 μM). Moreover, compound **44** (resistance factor value: 0.36) exhibited promising resistance to Bel-7402 cancer cells, lower than podophyllotoxin (resistance factor value: 0.84) and 5-Fu (resistance factor value: 16.83), which may be related to the ability of compound **44** to inhibit ERK1/2 phosphorylation levels.[78]

Derivative **45** (Fig. 6, Table 6, IC_{50}: 1.96–3.13 μM) exhibited broad-spectrum anti-tumor activity against HeLa and MCF-7

Table 6 Biological activity of podophyllotoxin-indole derivatives **44–49**

Compd.	Activity	Ref.
44	Bel-7402 cells: IC_{50} = 5.87 μM	66
45	HeLa cells: IC_{50} = 1.96 μM MCF-7 cells: IC_{50} = 3.13 μM	67
VP-16	HeLa cells: IC_{50} = 2.56 μM MCF-7 cells: IC_{50} = 8.61 μM	67
46	K562 cells: IC_{50} = 1.72 μM HeLa cells: IC_{50} = 3.92 μM	68
VP-16	K562 cells: IC_{50} = 6.26 μM HeLa cells: IC_{50} = 5.74 μM	68
47	K562 cells: IC_{50} = 1.13 μM HeLa cells: IC_{50} = 0.1 μM	69
VP-16	K562 cells: IC_{50} = 2.02 μM HeLa cells: IC_{50} = 1.98 μM	69
48	HeLa cells: IC_{50} = 0.79 μM	70
VP-16	HeLa cells: IC_{50} = 21.44 μM	70
49	K562 cells: IC_{50} = 0.4 μM HeLa cells: IC_{50} = 0.15 μM	71
VP-16	K562 cells: IC_{50} = 0.9 μM HeLa cells: IC_{50} = 2.11 μM	71

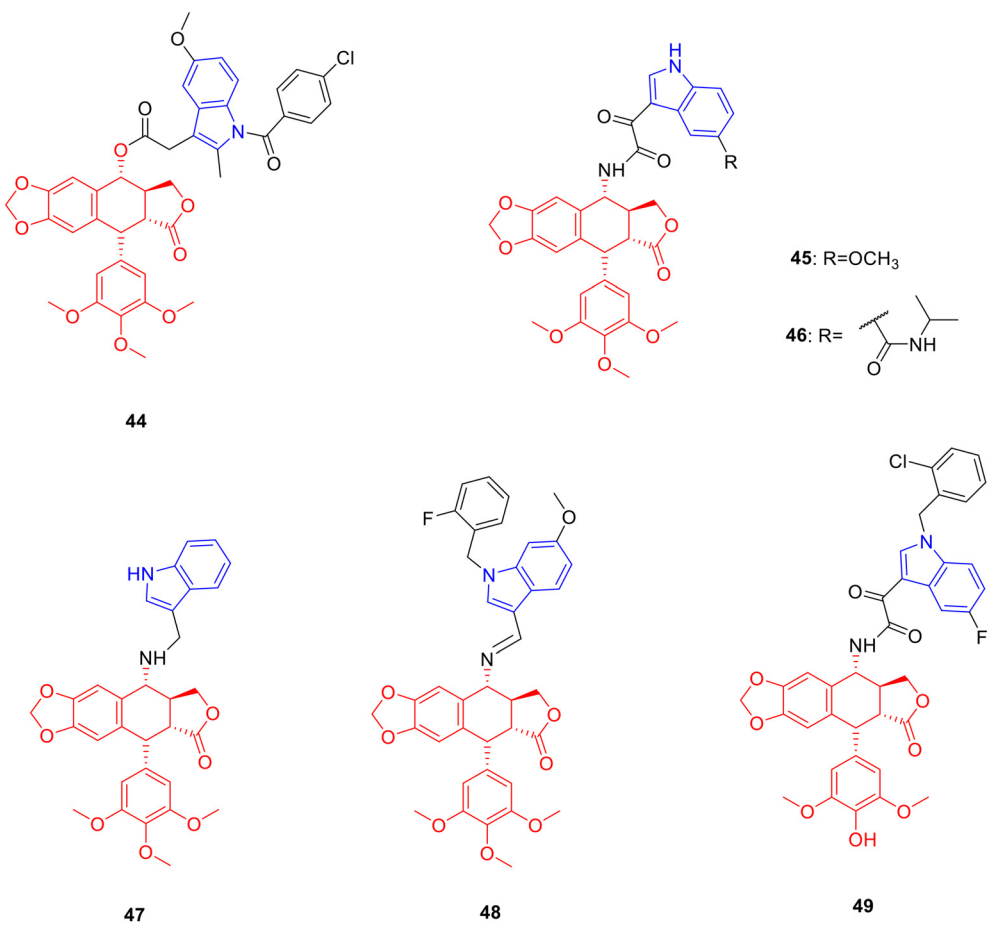

Fig. 6 Chemical structures of podophyllotoxin-indole derivatives **44–49**.

cancer cells, being more potent than VP-16 (IC_{50}: 2.56–8.61 μM). Mechanistic experiments showed that compound **45** achieved anti-tumor activity by inhibiting topoisomerase II and inducing apoptosis.[79]

Derivative **46** (Fig. 6, Table 6, IC_{50}: 1.72–3.92 μM) showed better anti-tumor activity against K562 and HeLa, stronger than VP-16 (IC_{50}: 5.74–6.26 μM). Although its anti-tumor activity against K562 was not as good as that of the parent podophyllotoxin (IC_{50}: 0.008 μM), it showed higher resistance to K562/A02 (resistance factor value: 0.73, resistance factor value of podophyllotoxin: 35), which could be further studied as a potential anti-tumor multidrug resistance drug.[80]

Derivative **47** (Fig. 6, Table 6, IC_{50}: 0.1–1.13 μM) showed considerable activity against HeLa and K562 cancer cells, being more potent than VP-16 (IC_{50}: 1.98–2.02 μM). The resistant factor of compound **47** (resistance factor value: 1.97) was lower than VP-16 (resistance factor value: 11.29) and the IC_{50} value of compound **47** (IC_{50}: 2.23 μM) against K562/AO2 was lower than VP-16 (IC_{50}: 22.81 μM), indicating that compound **47** possessed weak multidrug resistance.[81] Derivative **48** (Fig. 6, Table 6, IC_{50}: 0.79 μM) exhibited promising activity against HeLa cancer cells, being 27 fold more potent than VP-16 (IC_{50}: 21.44 μM).[82] Derivative **49** (Fig. 6, Table 6, IC_{50}: 0.15–0.4 μM) showed good activity against HeLa and K562 cancer cells, being more potent than VP-16 (IC_{50}: 0.9–2.11 μM).[83] Further research illustrated that the connection site of podophyllotoxin and the indole ring had a certain influence on the degree of anti-proliferative activity.

Coumarin is a lactone compound with a basic skeleton of the parent nucleus of benzo-alpha-pyrone, mainly distributed in *Apiaceae*, *Fabaceae*, *Asteraceae*, and *Ruta graveolens*, with anti-tumor,[84,85] anti-bacterial,[86] anti-leishmaniasis,[87] anti-oxidant,[88] hypoglycaemic,[89] anti-hyperlipidemia,[90] anti-Alzheimer's disease[91] and other pharmacological activities. Therefore, researchers modified the structure of coumarin, hoping to obtain new drugs with better biological activity. Derivative **50** (Fig. 7, Table 7, IC_{50}: 7.4 μM) exhibited significant anti-cancer activity against MCF-7 cancer cells as well as was lower cytotoxicity to VERO cells with an IC_{50} value >100 μM. SAR studies suggested that the introduction of aldehyde or carboxyl groups into the indole nucleus could enhance the anti-proliferative activity of compounds. Among them, compounds with halogen substitution in the coumarin ring exhibited better anticancer activity than the unsubstituted or hydroxy-substituted compounds, which may be due to the enhanced lipophilicity of the compounds by

Table 7 Biological activity of coumarin-indole derivatives **50–55**

Compd.	Activity	Ref.
50	MCF-7 cells: IC_{50} = 7.4 μM	79
51	MCF-7 cells: IC_{50} = 8.01 μM	80
52	MCF-7 cells: IC_{50} = 17.5 μM	81
53	HOP-92 cells: GI_{50} = 0.95 μM	82
54	MRSA: MIC = 0.25 μg mL^{-1}	83
	E. faecalis: MIC = 0.25 μg mL^{-1}	
	S. aureus ATCC 25922: MIC = 0.25 μg mL^{-1}	
	S. aureus ATCC 29213: MIC = 0.25 μg mL^{-1}	
	E. coli: MIC = 0.25 μg mL^{-1}	
	A. baumannii: MIC = 0.25 μg mL^{-1}	
Norfloxacin	MRSA: MIC = 4 μg mL^{-1}	83
	E. faecalis: MIC = 4 μg mL^{-1}	
	S. aureus ATCC 25922: MIC = 4 μg mL^{-1}	
	S. aureus ATCC 29213: MIC = 2 μg mL^{-1}	
	E. coli: MIC = 2 μg mL^{-1}	
	A. baumannii: MIC = 4 μg mL^{-1}	
55	*M. tuberculosis* H37Rv strain: MIC = 2.02 μM	84

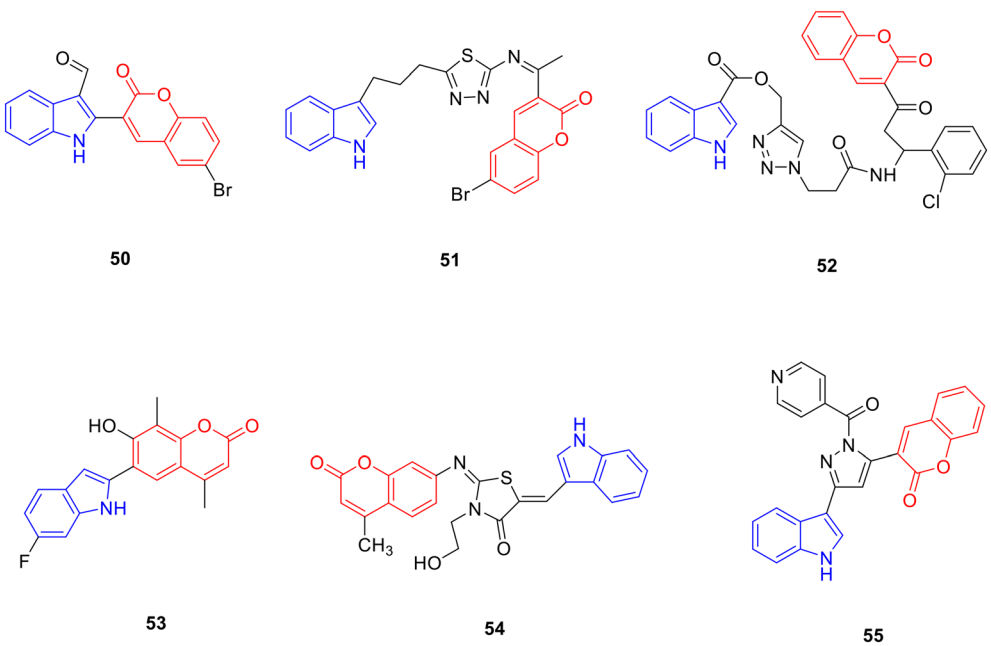

Fig. 7 Chemical structures of coumarin-indole derivatives **50–55**.

the halogen atoms. The presence of bromine atoms increased the anti-proliferative activity more than substitution with fluorine or chlorine atoms.[92]

Derivative **51** (Fig. 7, Table 7, IC_{50}: 8.01 μM) showed good anti-proliferative activity against MCF-7 cancer cells. The highest anti-proliferative activity was observed when the alkyl carbon chain length between the indole and thiazole rings was 3. The wound healing experiment showed that the migration ability of MCF-7 cells treated with compound **51** was significantly decreased, indicating that compound **51** can resist the metastasis of MCF-7 cancer cells.[93] Compound **52** (Fig. 7, Table 7, IC_{50}: 17.5 μM) showed considerable anti-proliferative activity to MCF-7 cancer cells, and the western blotting experiments showed that the expression level of CDK2 protein in cells was significantly decreased after compound **52** treatment.[94] Derivative **53** (Fig. 7, Table 7) exhibited good antimitotic activity, with a GI_{50} value of 0.95 μM.[95]

Derivative **54** (Fig. 7, Table 7) showed a broad antibacterial spectrum against methicillin-resistant *Staphylococcus aureus*, *Enterococcus faecalis*, *Staphylococcus aureus* ATCC 25922, *Staphylococcus aureus* ATCC 29213, *Escherichia coli* and *Acinetobacter baumannii* with a minimum inhibitory concentration (MIC) value of 0.25 μg mL^{-1}, and was potent more than norfloxacin (MIC: 2–4 μg mL^{-1}). SAR analysis showed that the introduction of the indole ring could greatly enhance the antibacterial activity of the compound, and the presence of the NH group of the indole ring was crucial for the antibacterial activity of the compound. Further studies showed that compound **54** caused the leakage of proteins, nucleic acids, and other substances by damaging the cell membrane of bacteria, thereby affecting their metabolism. Furthermore, compound **54** promotes excessive accumulation of intracellular ROS and induces lipid peroxidation to inhibit bacterial growth.[96]

The absence of substituents on the indole benzene ring or introduction of electron-withdrawing substituents can enhance the activity of the compounds. Derivative **55** (Fig. 7, Table 7, MIC: 12.5 μg mL^{-1}) showed good anti-tuberculosis activity to the *Mycobacterium tuberculosis* H37Rv strain (*M. tuberculosis* H37Rv strain);[97] derivatives **56** (Fig. 8, Table 8, IC_{50}: 95.5 μg mL^{-1}) and **57** (Fig. 8, Table 8, IC_{50}: 95 μg mL^{-1}) exhibited good anti-*Leishmania* activity. Furthermore, compound **56** and **57** also showed good anti-oxidant activity, and the IC_{50} values for anti-oxidant activity of compounds **56** and **57** were 12.4 μg mL^{-1} and 13.49 μg mL^{-1}, respectively. Their anti-*Leishmania* activity was approximately 5 fold more potent than that of sodium stibogluconate (IC_{50}: 490 μg mL^{-1}), and the anti-oxidant activity was comparable to that of sodium ascorbate (IC_{50}: 12.8 μg mL^{-1}).[98]

Derivative **58** (Fig. 8, Table 8, IC_{50}: 85 μM) displayed good inhibitory activity against α-glucosidase and was more potent than acarbose (IC_{50}: 750 μM). Enzyme kinetic experiments have shown that compound **58** inhibits α-glucosidase in a competitive manner.[99]

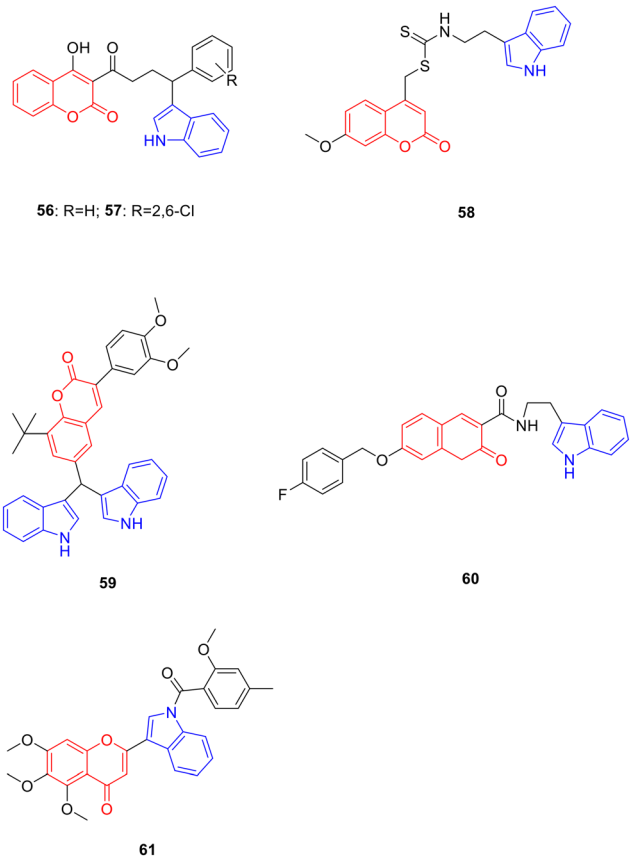

Fig. 8 Chemical structures of coumarin-indole derivatives **56**–**61**.

At a concentration of 10 μM, the inhibitory activity of derivative **59** (Fig. 8, Table 8, inhibition rate: 56%) against HMG-CoA reductase was comparable to that of atorvastatin (inhibition rate: 60%). *In vivo* experiments showed that compound **59** reduced the body weight of rats, reversed the levels of TC and TG in VLDL and LDL in hyperlipidaemic rats, and increased LCAT activity, LPL lipolytic activity, and receptor-mediated LDL catabolism to balance lipid metabolism.[100] In addition, the inhibitory activity SAR of derivative **60** (Fig. 8, Table 8, IC_{50}: 0.16 μM) against acetylcholinesterase illustrated that the benzyloxy group at

Table 8 Biological activity of coumarin-indole derivatives **56**–**60**

Compd.	Activity	Ref.
56	Anti-*Leishmania* activity: IC_{50} = 95.5 μg mL^{-1}	85
	DPPH: IC_{50} = 12.4 μM	
57	Anti-*Leishmania* activity: IC_{50} = 95 μg mL^{-1}	85
	DPPH: IC_{50} = 13.49 μM	
Sodium stibogluconate	Anti-*Leishmania* activity: IC_{50} = 490 μg mL^{-1}	85
Sodium ascorbate	DPPH: IC_{50} = 12.8 μM	85
58	α-Glucosidase: IC_{50} = 85 μM	86
Acarbose	α-Glucosidase: IC_{50} = 750 μM	86
59	HMG-CoA reductase: inhibition rate = 56%	87
60	Acetylcholinesterase: IC_{50} = 0.16 μM	88
61	HepG2 cells: IC50 = 4.63 μM	89
	SMMC-7721 cells: IC50 = 3.11 μM	

the C-7 position of coumarin is critical for activity.[101] Derivative **61** (Fig. 8, Table 8, IC_{50}: 3.11–4.63 μM) showed significant anti-proliferative activity against HepG-2 and SMMC-7721 cells. Further experiments showed that compound **8f** induced apoptosis in a concentration-dependent manner and down-regulated the expression of PKM2, PFKM, HK2 and tumor angiogenesis-related vascular endothelial growth factor.[102]

Cinnamic acid is an organic acid isolated from *Cinnamomum verum* bark that possesses anti-tumor,[103] anti-oxidant,[104] tyrosinase inhibitory[105] anti-bacterial[106] and other bioactivities. Pharmacochemistry researchers have modified the structure of cinnamic acid, hoping to obtain new drugs with research value such as anti-tumor, anti-oxidation and anti-bacterial activities. Derivative **62** (Fig. 9, Table 9, IC_{50}: 8.1 nM) exhibited comparable inhibitory activity against histone deacetylase enzyme and was potent more than vorinostat which served as the positive control (IC_{50}: 160.8 nM). The *in vitro* experiments showed that compound **62** (IC_{50}: 0.04–1.09 μM) exhibited good anti-proliferative activity on MOLT-4, HEL, K562, HeLa, and PC-3 cancer cells, being potent more than vorinostat (IC_{50}: 0.21–16.28 μM).[107]

Compared with the positive control, ferulic acid (ORAC value: 3.74), derivatives **63** (Fig. 9, Table 9, ORAC value: 8.71)[108] and **64** (Fig. 9, Table 9, ORAC value: 7.32)[109] showed higher stronger anti-oxidant activity and were 2.99 fold more potent than melatonin (ORAC value: 2.45), respectively. Derivative **65** (Fig. 9, Table 9) showed considerable DPPH radical scavenging activity with an EC_{50} value of 8.1 μM, which is more potent than ascorbic acid (EC_{50}: 23 μM).[110] Derivative **66** (Fig. 9, Table 9) exhibited good inhibitory against the *M. bovis* strain with 100 inhibition in 10 μg mL^{-1}. At a concentration of 30 μg mL^{-1}, derivative **67** (Fig. 9, Table 9) showed 90.4% inhibition against the *M. tuberculosis* strain, and rifampin was 99.5%.[111] Derivative **68** (Fig. 9, Table 9, IC_{50}: 50.98 μM) showed excellent DPPH radical scavenging activity, and was found to have a higher ability to neutralize free radical cation $ABTS^{\bullet+}$ than Trolox with an IC_{50} value of 19.49 μM, while the IC_{50} value of Trolox was 29.62 μM.[112]

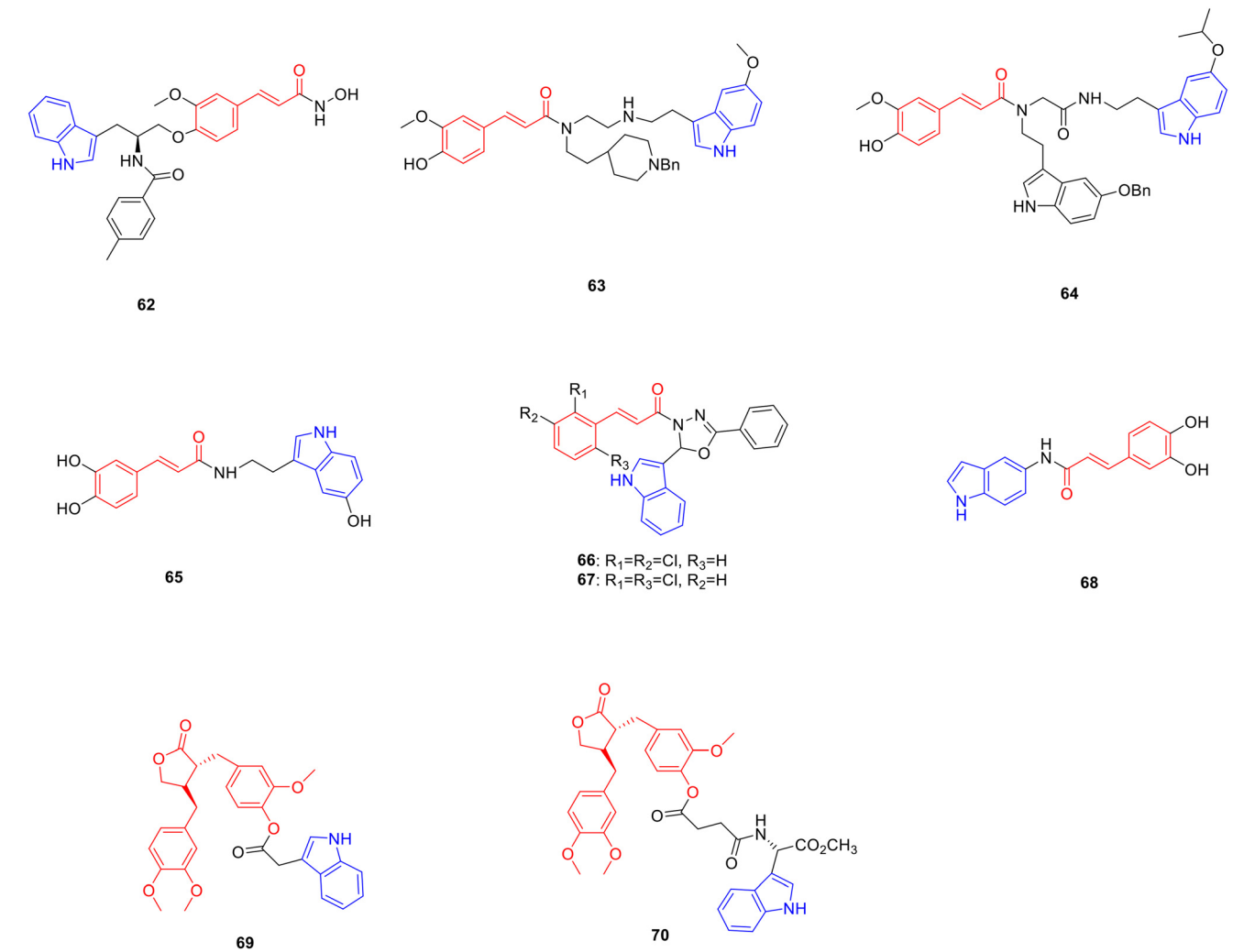

Fig. 9 Chemical structures of cinnamic-indole derivatives **62–68** and arctigenin-indole derivatives **69–70**.

Table 9 Biological activity of cinnamic-indole derivatives **62–68** and arctigenin-indole derivatives **69–70**

Compd.	Activity	Ref.
62	HeLa extract: IC_{50} = 8.1 nM MOLT-4 cells: IC_{50} = 0.04 μM HEL cells: IC_{50} = 0.15 μM K562 cells: IC_{50} = 0.32 μM HELA cells: IC_{50} = 0.31 μM PC-3 cells: IC_{50} = 1.09 μM	94
Vorinostat	HeLa extract: IC_{50} = 160 nM MOLT-4 cells: IC_{50} = 0.33 μM HEL cells: IC_{50} = 0.21 μM K562 cells: IC_{50} = 1.49 μM HELA cells: IC_{50} = 1.72 μM PC-3 cells: IC_{50} = 16.28 μM	94
63	ORAC value = 8.71	95
64	ORAC value = 7.32	96
Melatonin	ORAC value = 2.45	96
65	DPPH: EC_{50} = 8.1 μM	97
Ascorbic acid	DPPH: EC_{50} = 23 μM	97
66	*M. bovis* strain: inhibition rate = 100%	98
67	*M. tuberculosis* strain: inhibition rate = 90.4% Rifampin: inhibition rate = 99.5%	98
68	DPPH: IC_{50} = 50.98 μM	99
70	*T. gondii*-infected HeLa cells: IC_{50} = 187.2 μM	103
Arctigenin	*T. gondii*-infected HeLa cells: IC_{50} = 586.4 μM	103
Spiramycin	*T. gondii*-infected HeLa cells: IC_{50} = 262.2 μM	103

Arctigenin is a natural lignan product derived from the dried and ripe fruit of *Arctium lappa* and possesses anti-tumor[113] and anti-*T. gondii* activities.[114] Pharmacochemistry researchers have synthesized a series of arctigenin indole derivatives, expecting to obtain new drugs with research value such as anti-tumor and anti-Toxoplasma activities. In the H22 xenograft mouse model, derivative **69** (Fig. 9) showed significantly stronger inhibitory activity against tumour growth, and the tumour growth inhibitory rate was 45.04% at a dose of 40 mg kg^{-1}, which was more potent than arctigenin, with a tumour growth inhibitory rate of 27.86%. Serological data exhibited that compared with arctigenin (IL-2: 27.49 pg mL^{-1}; IL-6: 71.17 pg mL^{-1}; TNF-α: 59.86 pg mL^{-1}; IFN-γ: 40.07 pg mL^{-1}), the levels of IL-2, IL-6, TNF-α and IFN-γ in the serum of tumor-bearing mice treated with compound **69** (IL-2: 39.87 pg mL^{-1}; IL-6: 82.62 pg mL^{-1}; TNF-α: 70.65 pg mL^{-1}; IFN-γ: 45.17 pg mL^{-1}) were significantly increased at a dose of 40 mg kg^{-1}. In addition, at a dose of 40 mg kg^{-1}, the values of ALT, AST, BUN, and Cre in mice were comparable to those in the blank group, indicating that the high dose of compound **69** had little toxicity to the main functions of the liver and kidney in mice. Further study showed that compound **69** induced apoptosis, which may be related to the upregulation of BAX and Caspase-3 expression and the downregulation of Bcl-2 and VEGF expression.[115]

Derivative **70** (Fig. 9, Table 9, IC_{50}: 187.2 μM) exhibited promising anti-*T. gondii* activity and was potent more than arctigenin (IC_{50}: 586.4 μM) as well as spiramycin (IC_{50}: 262.2 μM). In addition, the selection index (SI) of compound **70** (SI: 3.2) was higher than that of arctigenin (SI: 0.98) and spiramycin (SI: 0.72), indicating that the introduction of the indole group enhanced the anti-*T. gondii* activity of arctigenin.[116]

Summary: indole-modified phenylpropanoid derivatives have been widely reported in podophyllotoxin, coumarin and cinnamic acid. The activity of podophyllotoxin-indole derivative **37** against HepG2, HeLa, A549 and MCF-7 tumor cells was more potent than podophyllotoxin as well as colchicine. When podophyllotoxin was attached to the C-4 position of the indole ring, toxicity was moderate. When it was attached to C-5 or C-6, the anti-proliferative activity of the compound was enhanced, whereas when it was attached to C-7 or C-2, the toxicity sharply decreased. Furthermore, the longer the alkyl chain attached to the indole, the less toxic the compound.

A variety of biological activities have been reported on indole-modified coumarin derivatives. The introduction of an aldehyde or carboxyl group in the indole nucleus can enhance the anti-proliferative activity of the compound, such as the IC_{50} of compound **50** was 7.4 μM, and the introduction of a benzyloxy group at the C7 position of the coumarin could increase the inhibitory activity of the compound against acetylcholinesterase, such as compound **60**. The nature of the linker between natural products and cinnamic acid also affects the activity of the compound. When the linker was benzamide, the activity was the strongest, and the substituent on the benzamide was an electron-donating group, which enhanced the activity of the compound more than the electron-withdrawing group. For example, cinnamic acid-indole derivative **62** showed nanomolar activity against histone deacetylase enzyme with an IC_{50} value of 8.1 nM.

5. Flavonoid-indole derivatives

Flavonoids are a series of compounds consisting of two phenolic hydroxyl groups interconnected by a central triple carbon atom, that is, compounds composed of C6–C3–C6 units, which have anti-tumor,[117] anti-inflammatory[118] and anti-bacterial activities.[119]

Chalcone is a flavonoid widely found in *Asteraceae*, *Fabaceae* and other plants, and possesses anti-tumor[120] and anti-bacterial activities.[121] Pharmacochemistry researchers worked on synthesizing chalcone linked indole derivatives in the hope to obtain promising anti-tumor and anti-bacterial drugs. Derivative **71** (Fig. 10, Table 10, IC_{50}: 0.84 μM) with an *N*1-methyl-substituted indole ring displayed considerable anti-proliferative activity against HepG2 cancer cells. In addition, the introduction of ester, alkoxy, and sulfonate groups also enhanced the anti-cancer activity. In particular, derivative **72** (Fig. 10, Table 10, IC_{50}: 0.22 μM) showed high anti-proliferative activity against HepG2 cancer cells, and low anti-proliferative activity against human normal cell line LO2 (IC_{50}: >10 μM). Mechanistic studies illustrated that compound **72** induced cancer cell arrest in the G2/M phase and apoptosis, and inhibited tubulin polymerisation. *In vivo* experiments showed that compound **72** showed significant

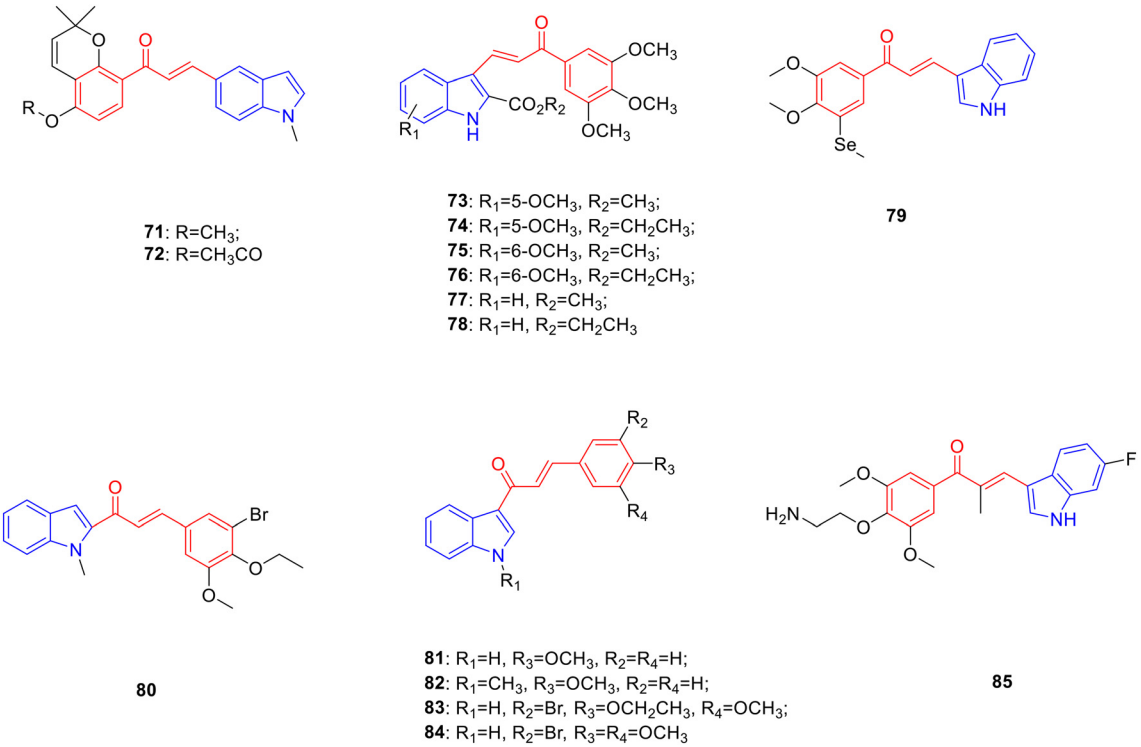

Fig. 10 Chemical structures of chalcone-indole derivatives **71**–**85**.

anti-tumor activity and had little effect on the growth of animals.[122]

Derivatives **73** (Fig. 10, Table 10, IC_{50}: 0.59–2.4 μM), **74** (Fig. 10, Table 10, IC_{50}: 0.33–0.46 μM), **75** (Fig. 10, Table 10, IC_{50}: 0.16–0.37 μM) and **76** (Fig. 10, Table 10, IC_{50}: 0.13–0.84 μM) exhibited promising anti-proliferative activity against HeLa, HT29 and MCF-7 cancer cell lines. The SAR showed that the position of the methoxy group introduced on the phenyl ring of the indole moiety had an important effect on anti-cancer activity. The anti-tumor activity of 5-methoxy-substituted compounds **73** and **74** and 6-methoxy-substituted compounds **75** and **76** was significantly stronger than compounds 77 (Fig. 10, Table 10, IC_{50}: 1.1–7.3 μM) and **78** (Fig. 10, Table 10, IC_{50}: 0.44–2.1 μM) without substituents on the benzene ring and the biological activity of 6-methoxy-substituted compounds was better than 5-methoxy-substituted compounds. Compound **74** exhibited stronger inhibitory activity against HeLa, HT29, and MCF-7 cancer cells than compound **73**, indicating that the introduction of ethoxycarbonyl at the C-2 position of indole had a more pronounced effect on promoting the anticancer activity of the compound. As mentioned above, the steric effect of the N1 position of the indole ring had a significant influence on biological activity. The introduction of alkyl, benzyl, and other substituents at the N1 position of the indole ring would reduce or even eliminate anti-cancer activity. Mechanistic studies showed that compounds **75** and **76** bound to the colchicine-binding domain to inhibit tubulin aggregation. Further experiments showed that compounds **74**, **75**, and **76** arrested the cell cycle in the G2/M phase and promoted apoptosis by inhibiting the JNK/SAPK pathway.[123]

Derivative **79** (Fig. 10, Table 10, IC_{50}: 0.023–0.059 μM) exhibited promising activity against HepG2, A549, and HeLa cancer cells.[124] Derivative **80** (Fig. 10, Table 10, IC_{50}: 4.3 μg mL^{-1}) showed promising activity against A549 cancer cells as well as being more potent than VP-16 (IC_{50}: 9.9 μg mL^{-1}). Further studies have shown that compound **80** may induce cell death by inhibiting the aggregation of tubulin, reducing mitochondrial thiol content, and inducing mitochondrial apoptosis.[125]

The SAR study showed that 4-methoxy-substituted chalcone-indole derivatives **81** (Fig. 10, Table 10, MIC: 4–8 μg mL^{-1}) and **82** (Fig. 10, Table 10, MIC: 1–8 μg mL^{-1}) had better inhibitory effects on *Trichophyton mentagrophytes*, *Microsporum fulvum*, and *Arthroderma benhamiae*. However, the antibacterial activity of the trimethoxy-substituted compounds did not improve, and indole *N*-methylation and *N*-ethylation did not improve the biological activity of the compounds. Interestingly, the antifungal activity of compounds substituted with bromine at the 3-position was generally better than that of trimethoxy-substituted compounds. The type of alkoxy group substituted on the benzene ring also affected the antibacterial activity of *Trichophyton verrucosum*, *T. mentagrophytes*, and *M. fulvum*. The antibacterial activity of compound **83** (Fig. 10, Table 10, MIC: 0.25–4 μg mL^{-1}) substituted by 4-ethoxy was 4–16 fold more potent than that of compound **84** (Fig. 10, Table 10, MIC: 1–32 μg mL^{-1}) obtained by 4-methoxy base-substitution.[126] Derivative **85** (Fig. 10, Table 10, IC_{50}: 3.2 nM)

Table 10 Biological activity of chalcone-indole derivatives 71–85

Compd.	Activity	Ref.
71	HepG2 cells: IC_{50} = 0.82 μM	109
72	HepG2 cells: IC_{50} = 0.22 μM	109
73	HeLa cells: IC_{50} = 2.4 μM HT29 cells: IC_{50} = 1 μM MCF-7 cells: IC_{50} = 0.59 μM	110
74	HeLa cells: IC_{50} = 0.33 μM HT29 cells: IC_{50} = 0.39 μM MCF-7 cells: IC_{50} = 0.46 μM	110
75	HeLa cells: IC_{50} = 0.37 μM HT29 cells: IC_{50} = 0.16 μM MCF-7 cells: IC_{50} = 0.17 μM	110
76	HeLa cells: IC_{50} = 0.84 μM HT29 cells: IC_{50} = 0.13 μM MCF-7 cells: IC_{50} = 0.24 μM	110
77	HeLa cells: IC_{50} = 2 μM HT29 cells: IC_{50} = 7.3 μM MCF-7 cells: IC_{50} = 1.1 μM	110
78	HeLa cells: IC_{50} = 2.1 μM HT29 cells: IC_{50} = 0.44 μM MCF-7 cells: IC_{50} = 1.8 μM	110
79	HepG2 cells: IC_{50} = 0.023 μM A549 cells: IC_{50} = 0.029 μM HeLa cells: IC_{50} = 0.059 μM	111
80	A549 cells: IC_{50} = 4.3 μg mL^{-1}	112
VP-16	A549 cells: IC_{50} = 9.9 μg mL^{-1}	112
81	*T. mentagrophytes*: MIC = 8 μg mL^{-1} *M. fulvum*: MIC = 4 μg mL^{-1} *A. benhamiae*: MIC = 8 μg mL^{-1}	113
82	*T. mentagrophytes*: MIC = 8 μg mL^{-1} *M. fulvum*: MIC = 1 μg mL^{-1} *A. benhamiae*: MIC = 4 μg mL^{-1}	113
83	*T. verucco*: MIC = 2 μg mL^{-1} *T. mentagrophytes*: MIC = 4 μg mL^{-1} *M. fulvum*: MIC = 0.25 μg mL^{-1}	113
84	*T. verucco*: MIC = 32 μg mL^{-1} *T. mentagrophytes*: MIC = 16 μg mL^{-1} *M. fulvum*: MIC = 1 μg mL^{-1}	113
85	HCT-116: IC_{50}: 3.2 nM	114

showed significant anti-proliferative activity against HCT-116 cells. *In vitro* experiments showed that compound **85** induced G2/M phase arrest by regulating the expression of cyclin B1, produced ROS, and targeted tubulin in HCT-116 cells. *In vivo* experiments showed that compound **85** could significantly inhibit tumor growth, which was higher than that of paclitaxel.[127]

Chrysin is a natural flavonoid present in the seeds and stem bark of *Oroxylum indicum* and has pharmacological activities such as anti-inflammatory and analgesic activities.[128] Researchers synthesized chrysin linked indole derivatives in the hope to obtain promising anti-inflammatory and analgesic drugs. Derivatives **86** (Fig. 11, Table 11, IC_{50}: 0.001–7 μM), **87** (Fig. 11, Table 11, IC_{50}: 0.007–60 μM) and **88** (Fig. 11, Table 11, IC_{50}: 0.07 μM) showed promising inhibitory activity against COX-2, being more potent than indomethacin (IC_{50}: 0.96 μM), and was comparable to bischlorothiophene (IC_{50}: 0.02 μM) as well as celecoxib (IC_{50}: 0.04 μM). Compared with COX-1, the inhibitory activities of compounds **86** and **87** against COX-2 were more obvious and exhibited certain selectivity. In particular, (*rac*) **86** (SI: 250) and (*S*) **86** (SI: 340) showed excellent COX-2 selectivity, with selectivity coefficients comparable to those of celecoxib (SI: 375). The SAR showed that the stereochemistry on the asymmetric carbon exhibited greater effect on the inhibition of COX-2 activity, and the compound with *S* configuration had more obvious anti-inflammatory activity, (*R*) **86** (IC_{50}: 7 μM) showed far less inhibitory effect against COX-2 than (*rac*) **86** (IC_{50}: 0.002 μM) and (*S*) **86** (IC_{50}: 0.001 μM), and (*R*) **87** (IC_{50}: 60 μM) exhibited lower anti-inflammatory activity than (*rac*) **87** (IC_{50}: 0.01 μM) and (*S*) **87** (IC_{50}: 0.007 μM) in the **87** series. The type of linker between indole and chrysin also affects the activity; compound (*S*) **87** with a linker of 2-propanol inhibited COX-2 10 times more than compound **88** (IC_{50}: 0.07 μM) with an alkyl chain as a linker. Further studies showed that compound (*S*) **86** might exert its anti-inflammatory effect by inhibiting the cyclooxygenase and lipoxygenase pathways.[129]

Derivative **89** (Fig. 11, Table 11, IC_{50}: 0.7 μM) showed promising inhibitory activity on COX-2, which was 36 fold more potent than chrysin (IC_{50}: 25.5 μM), and injection of 10 mg kg^{-1} of compound **89** into capsaicin-treated mice produced the same analgesic effect as 25 mg kg^{-1} of diclofenac. Hence, compound **89** has anti-inflammatory and analgesic potential, and merits further study.[130]

Xanthone is a benzochromone natural product, which mainly exists in microorganisms and has pharmacological activities such as antibacterial[131] and anti-inflammatory.[132] Chen *et al.* synthesized 23 xanthone derivatives and evaluated their antibacterial and anti-inflammatory activities. Derivative **90** (Fig. 11, Table 11, MIC: 15–22 μg mL^{-1}) showed good antibacterial activity against *Staphylococcus aureus* (*S. aureus*), *Bacillus subtilis* (*B. subtilis*), *E. coli* and *Klebsiella pneumonia* (*K. pneumonia*), being more potent than gentamicin (MIC: 26–28 μg mL^{-1}), and exhibited good antifungal activity against *Aspergillus niger* (*A. niger*), *Candida albicans* (*C. albicans*) and *Fusarium oxysporum* (*F. oxysporum*) (MIC: 20–21 μg mL^{-1}), being more potent than bavistin (MIC: 27–28 μg mL^{-1}). In addition, compound **90** (IC_{50}: 26 μg mL^{-1}) exhibited strong anti-inflammatory activity. Therefore, compound **90** has potential antibacterial and anti-inflammatory activities and deserves further investigation.[133]

Aurone is a natural product of flavonoids that contain a benzofuranone structure. It is a secondary product of plant metabolism, existing in *Scrophulariaceae*, *Asteraceae* and other plants, and has antiviral and other pharmacological activities.[134] Meguellati *et al.* modified the structure of the B-ring moiety of aurone. They designed and synthesized 37 new aurone derivatives in order to obtain drugs with better inhibitory effect on NS5B protein polymerase. Derivative **91** (Fig. 11, Table 11, IC_{50}: 2.4 μM) exhibited considerable inhibitory activity against NS5B protein polymerase, which was more potent than aurone (IC_{50}: 5.4 μM). Analysis of the SAR results showed that the indole group containing an unsubstituted benzene ring was very important for the enhancement of the anti-viral activity of aurone-indole derivatives. In addition, the introduction of benzyl and alkyl

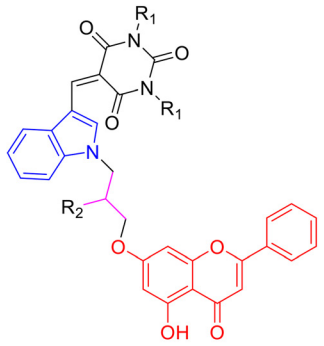

rac-**86**, *R*-**86**, *S*-**86**: R_1=H, R_2=OH
rac-**87**, *R*-**87**, *S*-**87**: R_1=CH_3, R_2=OH
88: R_1=R_2=CH_3

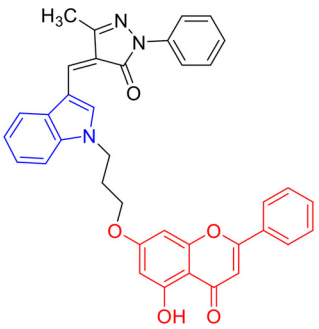

89

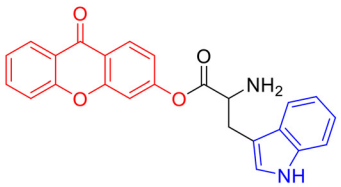

90

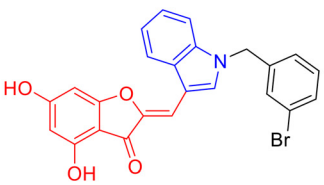

91

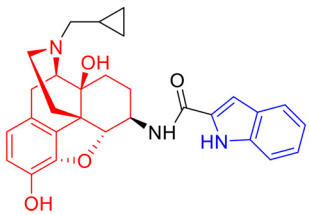

92

Fig. 11 Chemical structures of chrysin-indole derivatives **86**–**89**, xanthone-indole derivative **90**, aurone-indole derivative **91** and morphine-indole derivative **92**.

groups at the N1 position of the indole can enhance activity.[135]

Morphine, derived from the capsules of *Papaveraceae*, is a powerful opioid receptor regulator.[136] Obeng *et al.* synthesized 18 morphine indole derivatives, expecting to obtain new drugs with stronger binding ability to opioid receptors. Derivative **92** (Fig. 11) showed promising affinity for the mu opioid receptor, with an EC_{50} value of 0.21 nM. A warm water immersion assay showed that compound **92** was the opioid agonist with the highest antinociception.[137]

Summary: chalcone and chrysin-indole derivatives have good biological activities. Among them, chalcone-indole derivative **79** has strong anti-proliferative activity against HepG2, A549 and HeLa with IC_{50} values of 0.023 μM, 0.029 μM and 0.059 μM, respectively. The attachment site of chalcone to the indole ring was closely related to its anticancer activity. When chalcone was connected to the indole ring C-3 or C-5, the activity was the best; when it was connected to C-4 or C-6, the activity was moderate; and when it was connected to C-7, the activity decreased sharply. The steric effect of the N1 position of the indole ring is crucial for the anti-cancer activity; the larger the volume of the substituent on N1, the lower the anti-tumor activity. Chrysin-indole derivative (*S*) **87** has good anti-inflammatory activity with an IC_{50} of 0.007 μM. When the linker between indole and chrysin is isopropanol, the activity is stronger than that of alkyl.

6. Alkaloid-indole derivatives

Alkaloids are cyclic compounds containing nitrogen atoms in the negative oxidation state and are present in biological organisms. They are mainly classified into pyridine alkaloids, scopolamine alkaloids, isoquinoline alkaloids, indole alkaloids, and organic amine alkaloids, which have pharmacological activities such as anti-tumor activity.[138]

Sophoridine is a double-condensed piperidine alkaloid that exists in *Sophora alopecuroides* and has anti-tumor activity.[139] Researchers have designed and synthesized a series of sophoridine derivatives, hoping to obtain new drugs with excellent anti-tumor activity. Most sophoridine-indole derivatives showed considerable cytotoxic activity against HepG2 cancer cells, and the anti-proliferative activity of sophoridine derivatives modified with an indole group was much higher than that of sophoridine, indicating that the introduction of an indole group enhanced the anti-proliferative activity of sophoridine derivatives. Among them, derivative **93** (Fig. 12, Table 12, IC_{50}: 3.1 μM) showed considerable anti-proliferative activity against HepG2 cancer cells, which was potent more than the control drug camptothecin (IC_{50}: 13.2 μM) and lead compound

Table 11 Biological activity of chrysin-indole derivatives **86–89**, xanthone-indole derivative **90**, aurone-indole derivative **91** and morphine-indole derivative **92**

Compd.	Activity	Ref.
(*rac*) **86**	COX-2: IC_{50} = 0.002 μM	116
(*S*) **86**	COX-2: IC_{50} = 0.001 μM	116
(*R*) **86**	COX-2: IC_{50} = 7 μM	116
(*rac*) **87**	COX-2: IC_{50} = 0.01 μM	116
(*S*) **87**	COX-2: IC_{50} = 0.007 μM	116
(*R*) **87**	COX-2: IC_{50} = 60 μM	116
88	COX-2: IC_{50} = 0.07 μM	116
89	COX-2: IC_{50} = 0.7 μM	117
90	*S. aureus*: MIC = 16 μg mL^{-1}	120
	B. subtilis: MIC = 16 μg mL^{-1}	
	E. coli: MIC = 15 μg mL^{-1}	
	K. pneumonia: MIC = 22 μg mL^{-1}	
	A. niger: MIC = 21 μg mL^{-1}	
	C. albicans: MIC = 20 μg mL^{-1}	
	F. oxysporum: MIC = 20 μg mL^{-1}	
	Anti-inflammatory activity: IC_{50} = 26 μg mL^{-1}	
Gentamicin	*S. aureus*: MIC = 26 μg mL^{-1}	120
	B. subtilis: MIC = 28 μg mL^{-1}	
	E. coli: MIC = 26 μg mL^{-1}	
	K. pneumonia: MIC = 26 μg mL^{-1}	
Bavistin	*A. niger*: MIC = 27 μg mL^{-1}	120
	C. albicans: MIC = 28 μg mL^{-1}	
	F. oxysporum: MIC = 27 μg mL^{-1}	
91	NS5B protein polymerase: IC_{50} = 2.4 μM	122
Aurone	NS5B protein polymerase: IC_{50} = 5.4 μM	122
92	Mu opioid receptor: EC_{50} = 0.21 nM	124

sophoridine (IC_{50}: 4670 μM). The SAR analysis showed that the presence of an NH bond on indole N1 was not conducive to the anti-tumor activity, and substitution of benzyl and alkyl groups greatly enhanced the anti-tumor activity. When the ester group was substituted by an alcoholic hydroxyl group with better water solubility, the anti-tumor activity was stronger. Further experiments showed that compound **93** induced cell G1 arrest and inhibited topoisomerase I in the human hepatocellular carcinoma xenograft mouse model; treatment with compound **93** at 40 mg kg^{-1} resulted in a significant inhibition of tumour growth with a *T*/*C* value of 55.99% without loss of body weight, while the sophoridine group induced 93.38%. Therefore, compound **93** deserves further study as a potential anti-tumor drug agent.[140]

Derivative **94** (Fig. 12, Table 12, IC_{50}: 0.93–1.44 μM) exhibited promising anti-tumor activity against HepG2, SMMC-7721, HeLa and MCF-7 cancer cell lines. The anti-proliferative activity of HpeG2 cells was stronger than that of camptothecin (IC_{50}: 1.36 μM). The results of the SAR analysis indicated that the α,β-unsaturated ketone structure in sophoridine derivatives was important for cytotoxic activity. When the C-5 or C-6 position of the indole ring was replaced by –Me, –Cl, and –Br, the cytotoxic activity decreased, and when the C-5 position of the indole ring was replaced by $–OCH_3$, the cytotoxic activity was enhanced. The results of the enzymatic assay showed that compound **94** inhibited topoisomerase I activity. In addition, activation of caspase-3 and reduction of the Bcl-2/Bax ratio suggest that this compound may be a potential anticancer agent.[141]

Matrine is a double-condensed piperidine alkaloid derived from the dried root of *Sophora flavescens* and has anti-tumor

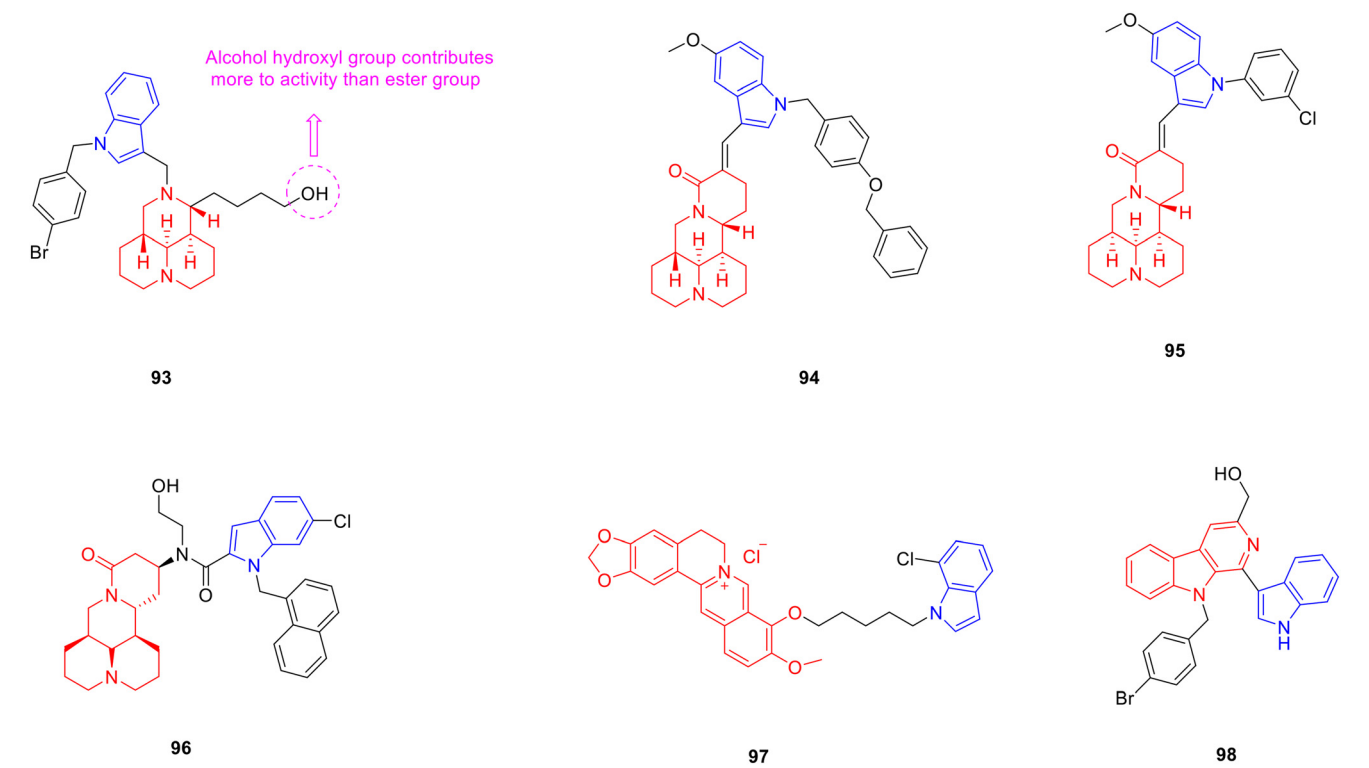

Fig. 12 Chemical structures of alkaloid-indole derivatives **93–98**.

Table 12 Biological activity of alkaloid-indole derivatives **93–98**

Compd.	Activity	Ref.
93	HepG2 cells: IC_{50} = 3.1 μM	127
Camptothecin	HepG2 cells: IC_{50} = 13.2 μM	127
Sophoridine	HepG2 cells: IC_{50} = 4670 μM	127
94	HepG2 cells: IC_{50} = 0.93 μM SMMC-7721 cells: IC_{50} = 1.32 μM HeLa cells: IC_{50} = 1.44 μM MCF-7 cells: IC_{50} = 0.94 μM	128
Camptothecin	HepG2 cells: IC_{50} = 1.36 μM	128
95	SMMC-7721 cells: IC_{50} = 3.95 μM A549 cells: IC_{50} = 4.96 μM	130
Matrine	SMMC-7721 cells: IC_{50} = 6591 μM A549 cells: IC_{50} = 5725 μM	130
Cisplatin	SMMC-7721 cells: IC_{50} = 6.08 μM A549 cells: IC_{50} = 8.56 μM	130
96	HeLa cells: IC_{50} = 0.9 μM MCF-7 cells: IC_{50} = 1.2 μM SGC-7901 cells: IC_{50} = 1.1 μM HepG2 cells: IC_{50} = 1.2 μM	131
97	DPPH: IC_{50} = 17.09 μg mL^{-1}	133
Berberine	DPPH: IC_{50} = 41.87 μg mL^{-1}	133
98	*S. aureus*: MIC = 3.125 μg mL^{-1} MRSA: MIC = 3.125 μg mL^{-1} *B. cereus*: MIC = 3.125 μg mL^{-1} *R. solanacearum*: MIC = 1.5625 μg mL^{-1}	135
Fosfomycin sodium	*S. aureus*: MIC = 100 μg mL^{-1} MRSA: MIC = 50 μg mL^{-1} *B. cereus*: MIC = 25 μg mL^{-1} *R. solanacearum*: MIC = 50 μg mL^{-1}	135

activity.[142] Researchers designed and synthesized a series of matrine derivatives and evaluated the anti-tumor activity of these compounds. Derivative **95** (Fig. 12, Table 12, IC_{50}: 3.95–4.96 μM) showed considerable anti-proliferative activity against SMMC-7721 and A549 cancer cells, being more potent than matrine (IC_{50}: 5725–6591 μM) and cisplatin (IC_{50}: 6.08–8.56 μM). Further studies showed that compound **95** induced apoptosis of CNE2 and SMMC-7721 cells in a dose-dependent manner. Therefore, compound **95** is worthy of further exploration as a potential anti-tumor drug.[143] Derivative **96** (Fig. 12, Table 12, IC_{50}: 0.9–1.2 μM) showed strong anti-proliferative activity against HeLa, MCF-7, SGC-7901, HepG2 cancer cell lines and was 3 orders of magnitude stronger than matrine. Further studies demonstrated that compound **96** strongly induced mitochondrial stress, manifested as impaired energy metabolism, mitochondrial membrane potential depolarization, mitochondrial calcium overload and increased ROS production. SAR analysis showed that the properties of the substituents on the indole ring had a great influence on the antiproliferative activity of the compounds, and the activity sequence was: 6-Cl > 6-Br > 6-Me > 6-F > 6-OCH_3.[144]

Berberine is a quaternary ammonium alkaloid derived from the rhizome of *Coptis chinensis* that has anti-oxidant activity.[145] Mistry *et al.* combined a variety of heterocyclic nitrogen nuclei in the form of indole structural units with berberine to obtain new drugs with better antioxidant activity. They synthesized 10 different types of berberine-indole derivatives. The anti-oxidant activity of derivative **97** (Fig. 12, Table 12, IC_{50}: 17.09 μg mL^{-1}) was comparable to that of ascorbic acid (IC_{50}: 15.59 μg mL^{-1}), and was stronger than berberine (IC_{50}: 41.87 μg mL^{-1}). Therefore, compound **97** could be further studied as a novel anti-oxidant.[146]

Carboline is an alkaloid with a tricyclic structure, formed by the fusion of a pyridine ring with the pyrrole ring of an indole. Dai *et al.* designed and synthesized 32 carboline-indole derivatives with different substituents, expecting to obtain new drugs with good antibacterial activity. It was first discovered in the seeds of *Peganum harmala* and exhibited good antibacterial activity.[147] Derivative **98** (Fig. 12, Table 12, MIC: 3.125–1.56 μmol L^{-1}) was more potent than fosfomycin sodium (MIC: 25–100 μmol L^{-1}) against *S. aureus*, MRSA, *Bacillus cereus* (*B. cereus*) and *Ralstonia solanacearum* (*R. solanacearum*). Further studies implied that compound **98** damages the cell membrane and increases permeabilization.[148]

Summary: sophoridine, matrine, and berberine indole derivatives all showed stronger biological activity than their parent compounds, among which are derivatives **93**, **95**, **96**. The anti-tumor activity of these derivatives was stronger than that of the parent by three orders of magnitude. Therefore, compounds **93**, **95**, **96** were worthy of further study.

7. Steroid-indole derivatives

Steroids are a class of naturally widespread chemical components, a class of compounds containing cyclopentanoperhydrophenanthrene, including phytosterols, bile acids, C21 steroids, steroid saponins, *etc.*, which have pharmacological activities such as anti-tumor,[149] anti-Alzheimer's disease,[150] and α-glucosidase activity inhibition.[151]

Lithocholic acid is a secondary bile acid, also known as cholelithic acid, which is produced by the bacterial metabolism of chenodeoxycholic acid in the intestine and has anti-tumor activity.[152] Most researchers have modified the carboxyl group of lithocholic acid, and they have synthesized many lithocholic acid-indole derivatives, hoping to obtain antitumor drugs with research prospects. Derivative **99** (Fig. 13, Table 13, IC_{50}: 0.8 μM) showed significant inhibitory activity against the EphA2 receptor, which was about 98 fold more potent than lithocholic acid (IC_{50}: 79 μM). SAR analysis revealed that free carboxyl groups are critical for the ability of the compound to inhibit EphA2-ephrin-A1 binding. The introduction of a single aryl group to the compound did not improve its inhibitory activity. In contrast, the introduction of heterocycles, such as naphthalene rings, indole rings, and benzothiophenes, improved the inhibitory activity. Since the NH group on the indole ring can form weak hydrogen bonds with the EphA2 receptor, the compounds with the indole ring showed a strong ability to inhibit the binding of EphA2-ephrin-A1 among the tested compounds. In a pharmacokinetic study, compound **99** not only had good solubility and plasma stability, but also had high metabolic stability, which may be

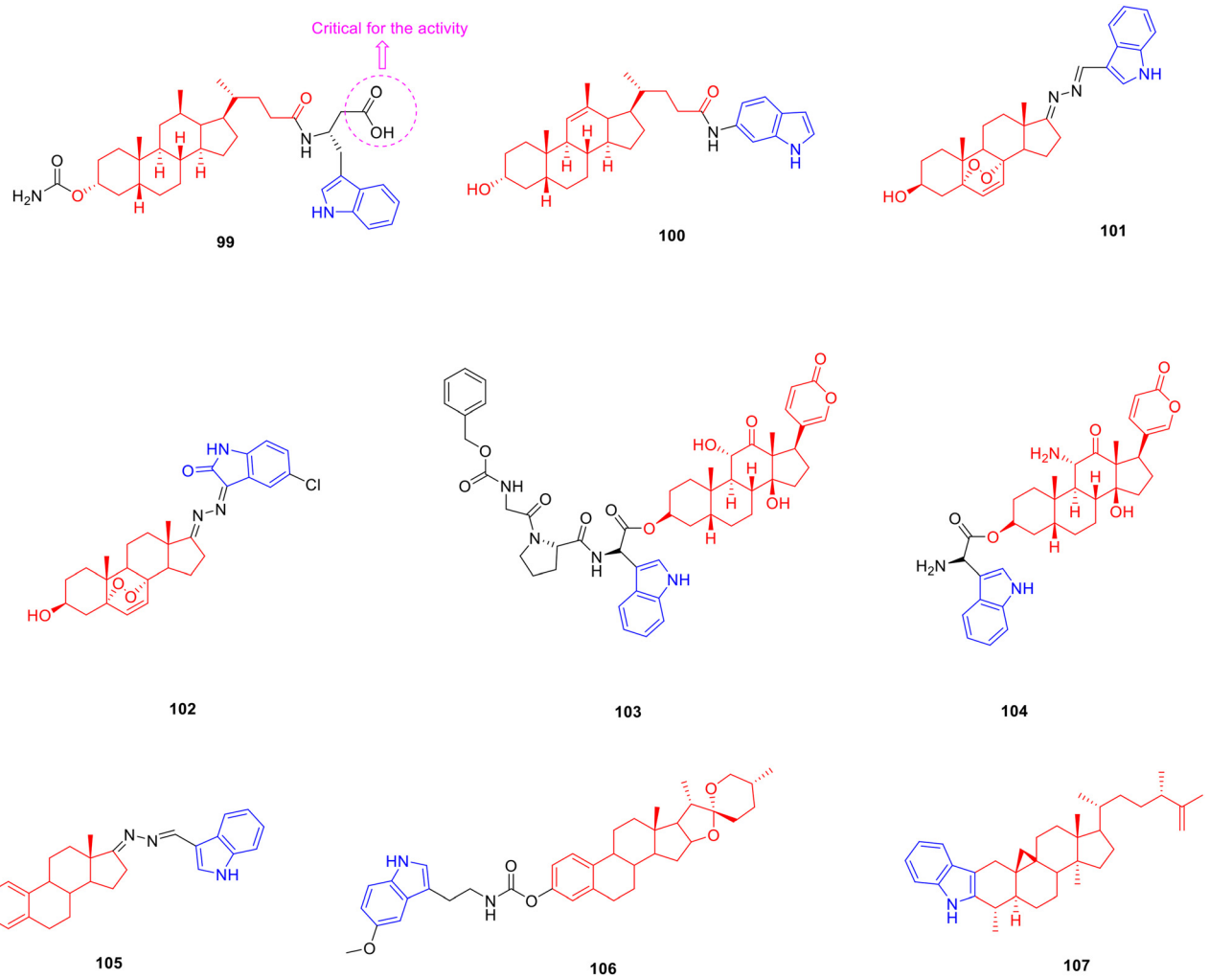

Fig. 13 Chemical structures of steroid-indole derivatives **99**–**107**.

related to the fact that the acyloxy group at the C-3 position of compound **99** is not easily oxidised.[153]

Derivative **100** (Fig. 13, Table 13, IC_{50}: 8.8 μM) showed considerable anti-proliferative activity against MCF-7 cells, which was comparable to that of the positive control drug tamoxifen (IC_{50}: 7.05 μM), and was more potent than the parent lithocholic acid (IC_{50}: 150.3 μM). Compound **100** (IC_{50}: 4.28 μM) was also able to reverse the multidrug resistance of MCF-7/ADR cells. In addition, the presence of the alkenyl group at the C-11 position can significantly improve anti-tumor activity.[154]

Ergosterol is a plant sterol compound widely distributed in fungi, with anti-tumor activity.[155] Researchers have devoted themselves to the synthesis of indole derivatives linked to ergosterol and evaluated the anti-tumor activity of these derivatives. The SAR showed that derivative **101** (Fig. 13 , Table 13, IC_{50}: 9.38–15.78 μM) containing an indole structure exhibited promising anti-proliferative activity against HepG2, SK-Hep1, MCF-7 and MDA-MB-321 cancer cell lines, being more potent than parental ergosterol (IC_{50}: 16.8–23.31 μM).[156] Derivative **102** (Fig. 13, Table 13, IC_{50}: 5.69–9.05 μM) displayed considerable anti-proliferative activity against HepG2, MCF-7 and HeLa cancer cell lines, being more potent than ergosterol (IC_{50}: 18.00–23.35 μM). In addition, the presence of electron-withdrawing groups on the indole ring contributed more to the anti-tumor activity than the electron-withdrawing groups. Further experiments showed that compound **102** induced G1 phase arrest and inhibited colony growth in HepG2 cells. Therefore, compound **102** can be used as a lead compound for anti-tumor agents, which is worthy of further study.[157]

Arenobufagin is a cardiac glycoside steroid derived from the dry secretions of *Bufo gargarizans* and has anti-tumor activity.[158] Researchers have designed and synthesized a series of arenobufagin-indole derivatives, hoping to obtain new drugs with good anti-tumor activity. Derivative **103** (Fig. 13, Table 13, V_{max}: 0.682 μmol min^{-1} mg^{-1}, S50: 10.36 μmol L^{-1}, CL int: 65.89 mL min^{-1} mg^{-1}) is a prodrug activated by the FAPα enzyme which is only expressed in tumour tissues. Further study revealed that compound **103** could be cleaved by hFAPα with the highest enzymatic hydrolysis efficiency among arenobufagin-indole derivatives.

Table 13 Biological activity of steroid-indole derivatives **99–107**

Compd.	Activity	Ref.
99	EphA2 receptor: IC_{50} = 0.8 μM	140
Lithocholic acid	EphA2 receptor: IC_{50} = 79 μM	140
100	MCF-7 cells: IC_{50} = 8.8 μM	141
	MCF-7/ADR cells: IC_{50} = 4.28 μM	
Lithocholic acid	MCF-7 cells: IC_{50} = 150.03 μM	141
101	HepG2 cells: IC_{50} = 10.63 μM	143
	SK-Hep1 cells: IC_{50} = 9.38 μM	
	MCF-7 cells: IC_{50} = 15.78 μM	
	MDA-MB-231 cells: IC_{50} = 10.66 μM	
Ergosterol	HepG2 cells: IC_{50} = 16.8 μM	143
	SK-Hep1 cells: IC_{50} = 17.25 μM	
	MCF-7 cells: IC_{50} = 23.31 μM	
	MDA-MB-231 cells: IC_{50} = 19.17 μM	
102	HepG2 cells: IC_{50} = 7.97 μM	144
	MCF-7 cells: IC_{50} = 9.05 μM	
	HeLa cells: IC_{50} = 5.69 μM	
Ergosterol peroxide	HepG2 cells: IC_{50} = 23.35 μM	144
	MCF-7 cells: IC_{50} = 18.00 μM	
	HeLa cells: IC_{50} = 19.54 μM	
104	MDA-MB-453 cells: IC_{50} = 10.64 nM	146
	MCF-7 cells: IC_{50} = 11.6 nM	
	MDA-MB-231 cells: IC_{50} = 27.00 nM	
105	MDA-MB-453 cells: IC_{50} = 10.01 nM	146
	MCF-7 cells: IC_{50} = 1.06 nM	
	MDA-MB-231 cells: IC_{50} = 4.81 nM	
106	HeLa cells: IC_{50} < 5 μM	148
Cisplatin	HeLa cells: IC_{50} = 10 μM	148
107	α-Glucosidase: IC_{50} = 115.2 μM	151
Cyclomusalenone	α-Glucosidase: IC_{50} = 603.8 μM	151
Acarbose	α-Glucosidase: IC_{50} = 420.2 μM	151

Furthermore, compound **103** (IC_{50}: 10.64–27.00 nM) exhibited considerable activity comparable to that of the lead product arenobufagin (IC_{50}: 8.88–22.45 nM) against MDA-MB-435, MCF-7, and MDA-MB-231 cancer cell lines and displayed significantly reduced cardiotoxicity. More importantly, the active form of compound **104** (Fig. 13, Table 13, IC_{50}: 1.06–10.01 nM) showed strong activity against MDA-MB-435, MCF-7, and MDA-MB-231 cells. In the MDA-MB-231 xenografted mouse model, compound **103** exhibited a tumor regression effect at a dose of 12 μmol kg^{-1} with tumors weighing 0.43 ± 0.18 g, while the control group was 0.67 ± 0.14 g. Hence, compound **103** provides a new candidate drug for alleviating cardiotoxicity of clinical anti-cancer drugs.[159]

Dehydroepiandrosterone is a C_{21} steroid, an intermediate in testosterone biosynthesis, with anti-tumor activity.[160] Cui *et al.* synthesized a series of dehydroepiandrosterone derivatives with different aromatic heterocyclic structures at the 17-position side chain of the steroid nucleus and evaluated their anti-tumor activity. Derivative **105** (Fig. 13, Table 13, IC_{50}: <5 μM) showed good anti-proliferative activity against HeLa cells and was stronger than cisplatin (IC_{50}: 10 μM).[161]

Diosgenin is a steroidal saponin, which is widely present in the tubers of Dioscoreaceae plants, such as *Discorea nipponica* and *Dioscorea zingiberensis*, possessing neuroprotective activity.[162] Zhou *et al.* designed and synthesized 10 diosgenin derivatives linked to indole groups, expecting to obtain new drugs for multi-target anti-Alzheimer's disease. At a concentration of 10 μM, derivative **106** (Fig. 13, Table 13, cell viability: 52.9–54.4%) exhibited considerable neuroprotective activity against H_2O_2 and Aβ injury. The SAR results showed that the properties of the benzene ring substituents were closely related to the enhanced anti-oxidant activities of the compounds. The active sequence of substituents on the benzene ring was as follows: 5-OCH_3 > 5-CH_3 > 5-F > 5-Cl > 5-Br > 5-H. The introduction of a methoxy group has a stronger effect on activity enhancement than the introduction of a methyl group, which may be caused by the conjugation of the methoxy group and indole ring. Substitution of C-5 of the indole ring is beneficial for enhancing neuroprotective activity. In addition, carbamates are significantly more effective than esters as linkers between indole and diosgenin. *In vivo* studies showed that compound **106** improved spatial memory and learning impairment in mice injected with Aβ. Overall, compound **106** is a potential anti-Alzheimer's agent with neuroprotective activity that deserves further study.[163]

Cyclomusalenone is found in the peel of *Musa balbisiana* and has hypoglycaemic activity. Smirnova *et al.* designed and synthesized a series of cyclomusalenone derivatives, expecting to obtain hypoglycemic drugs with research value. Derivative **107** (Fig. 13, Table 13, IC_{50}: 115.2 μM) was an effective inhibitor of α-glucosidase being 5.2-and-3.6 fold more active than cyclomusalenone and acarbose.[164]

Summary: compounds **99** and **100** showed strong anti-tumor activity with IC_{50} values of 0.8 μM and 8.8 μM, respectively, which were 98 and 17 times stronger than the parent. The carboxyl group on the linker between lithocholic acid and indole enhanced the activity of compound **100**,

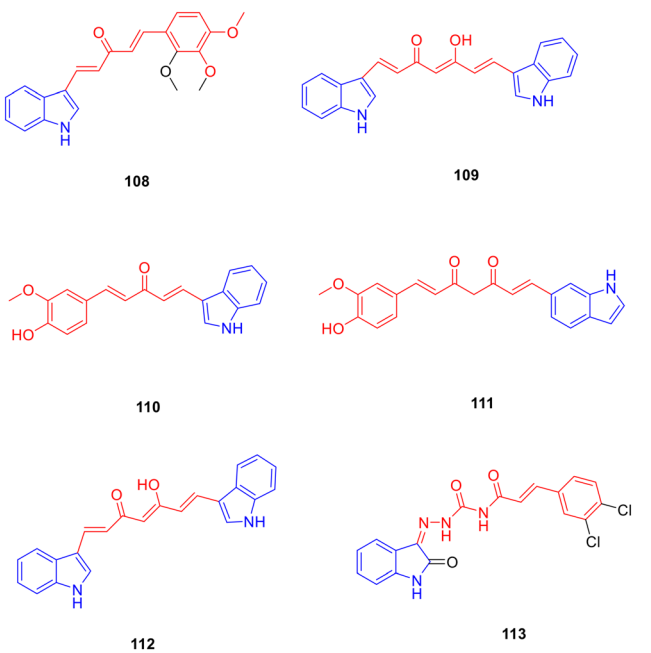

Fig. 14 Chemical structures of curcumin-indole derivatives **108–113**.

Table 14 Biological activity of curcumin-indole derivatives **108–113**

Compd.	Activity	Ref.
108	PC-3 cells: IC_{50} = 3.15 μM HeLa cells: IC_{50} = 3.31 μM	158
Curcumin	PC-3 cells: IC_{50} = 12.22 μM HeLa cells: IC_{50} = 25.41 μM	158
109	Caco-2 cells: IC_{50} = 3.3 μM CHO-K1 cells: IC_{50} = 7.9 μM	159
Curcumin	Caco-2 cells: IC_{50} = 28 μM CHO-K1 cells: IC_{50} = 21.3 μM	159
110	Caco-2 cells: IC_{50} = 8 μM	160
Curcumin	Caco-2 cells: IC_{50} = 47.6 μM	160
111	Aβ: IC_{50} = 0.42 μM Tau: IC_{50} = 0.44 μM	161
Curcumin	Aβ: IC_{50} = 5.4 μM Tau: IC_{50} = 3 μM	161
112	Hep 3B: IC_{50} = 14 μM	162
113	IL-6: 1.06 μM	163

while compounds **103** and **104** showed nanomolar anti-proliferative activity against MDA-MB-435, MCF-7, and MDA-MB-231, so compounds **99**, **100**, **103** and **104** were valuable compounds for research.

8. Polyphenol-indole derivatives

Polyphenols are a collective name for a group of chemicals in plants, named for having multiple phenolic groups, with pharmacological activities, such as anti-tumor,[165] anti-Alzheimer's disease[166] and anti-inflammatory.[167]

Curcumin is a polyphenolic compound extracted from the rhizome of *Curcuma longa* and has anti-tumor,[168] anti-Alzheimer's disease[169] and anti-inflammatory activities.[170] Researchers have designed and synthesized many curcumin-indole derivatives, expecting to obtain anti-tumor, anti-Alzheimer's disease and anti-inflammatory drugs with good biological activity. Derivative **108** (Fig. 14, Table 14, IC_{50}: 3.15–3.31 μM) showed strong anti-tumor activity against PC-3 and HeLa cancer cell lines, being more potent than curcumin (IC_{50}: 12.22–25.41 μM). Further research revealed that

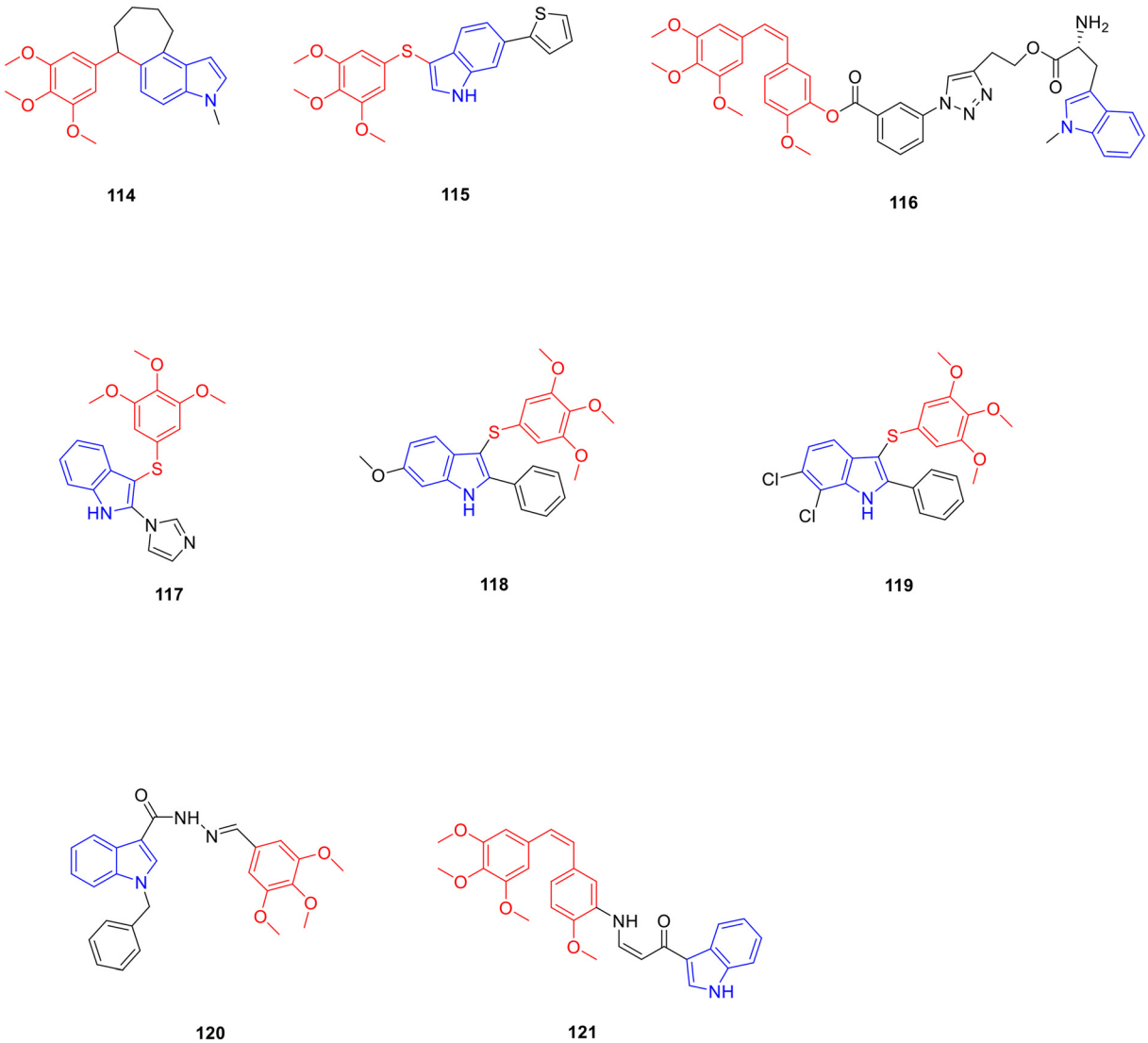

Fig. 15 Chemical structures of resveratrol-indole derivatives **114–121**.

compound **108** significantly inhibited tubulin polymerisation, reduced the mitochondrial inner membrane, induced cell G2/M cycle arrest and apoptosis. In addition, the presence of electron-donating groups on the benzene ring is important for anti-tumor activity.[171]

Derivative **109** (Fig. 14, Table 14, IC_{50}: 3.3–7.9 μM) showed promising broad-spectrum anti-tumor activity against Caco-2 and CHO-K1 cancer cell lines, being more potent than curcumin (IC_{50}: 21.3–28 μM). Further experiments indicated that compound **109** might induce apoptosis through the accumulation of ROS in tumour cells.[172]

Replacing the phenyl moiety of curcumin with an indole group is important for enhancing the Caco-2 inhibitory activity of curcumin and the pharmacological activity of curcumin against Alzheimer's disease. Derivative **110** (Fig. 14, Table 14, IC_{50}: 8 μM) showed promising anti-tumor activity against Caco-2 cancer cells, being 6 fold more potent than curcumin (IC_{50}: 47.6 μM).[173] Derivative **111** (Fig. 14, Table 14, IC_{50}: 0.42–0.44 μM) exhibited considerable inhibitory activity against Aβ and tau protein aggregation, being 8–10 fold more potent than curcumin (IC_{50}: 3.0–5.4 μM).[174] Derivative **112** (Fig. 14, Table 14, IC_{50}: 14 μM) showed strong anti-proliferative activity against Hep3B cancer cells, inhibiting cell migration in a time- and dose-dependent manner and decreasing MMP-9 activity.[175] Derivative **113** (Fig. 14, Table 14, IC_{50}: 1.05 μM) showed strong inhibitory activity against IL-6, which was superior to curcumin and indomethacin and had no obvious cytotoxic side effects. Further experiments showed that compound **113** significantly inhibited LPS-induced inflammatory response, reduced the number of neutrophils and lung wet-to-dry weight ratio. Therefore, compound **11** is a promising anti-inflammatory drug.[176]

Table 15 Biological activity of resveratrol-indole derivatives **114–121**

Compd.	Activity	Ref.
114	A549 cells: IC_{50} = 0.022 μM HeLa cells: IC_{50} = 0.056 μM PC-3 cells: IC_{50} = 0.047 μM Bel-7402 cells: IC_{50} = 0.039 μM Lovo cells: IC_{50} = 0.049 μM A2780 cells: IC_{50} = 0.037 μM MCF-7 cells: IC_{50} = 0.051 μM	165
115	MV4-11 cells: IC_{50} = 6 nM THP-1 cells: IC_{50} = 2 nM A549 cells: IC_{50} = 2 nM PC-3 cells: IC_{50} = 3.5 nM	166
116	HeLa cells: IC_{50} = 0.07 μM	167
CA-4	HeLa cells: IC_{50} = 0.21 μM	167
117	HT-29 cells: IC_{50} = 0.03 μM A549 cells: IC_{50} = 0.02 μM	168
CA-4	HT-29 cells: IC_{50} = 0.13 μM A549 cells: IC_{50} > 10 μM	168
118	MDA-MB-468 cells: IC_{50} = 37 nM MDA-MB-436 cells: IC_{50} = 62 nM MDA-MB-23 cells: IC_{50} = 39 nM PC-3 cells: IC_{50} = 0.3 nM RD cells: IC_{50} = 0.2 nM HepG2 cells: IC_{50} = 0.1 nM	169
119	MDA-MB-468 cells: IC_{50} = 33 nM MDA-MB-436 cells: IC_{50} = 75 nM MDA-MB-23 cells: IC_{50} = 47 nM PC-3 cells: IC_{50} = 19 nM RD cells: IC_{50} = 16 nM HepG2 cells: IC_{50} = 62 nM	169
Vinblastine	PC-3 cells: IC_{50} = 766 nM RD cells: IC_{50} = 53 nM HepG2 cells: IC_{50} = 81 nM	169
Paclitaxel	PC-3 cells: IC_{50} = 4900 nM RD cells: IC_{50} > 10 000 nM HepG2 cells: IC_{50} = 2600 nM	169
120	HepG2 cells: IC_{50} = 0.63 μM HeLa cells: IC_{50} = 5.89 μM MCF-7 cells: IC_{50} = 0.64 μM A549 cells: IC_{50} = 0.08 μM	170
121	A549 cells: IC_{50} = 0.015 μM HeLa cells: IC_{50} = 0.053 μM MCF-7 cells: IC_{50} = 0.031 μM HCT116 cells: IC_{50} = 0.033 μM	171
CA-4	A549 cells: IC_{50} = 0.031 μM HeLa cells: IC_{50} = 0.058 μM MCF-7 cells: IC_{50} = 0.058 μM HCT116 cells: IC_{50} = 0.398 μM	171

Resveratrol, a polyphenolic natural product, was first isolated from the roots of *Veratrum grandiflorum* in 1940 and has anti-tumor pharmacological activity.[177] Many resveratrol-indole derivatives have been synthesized by researchers, who expect to obtain anti-tumor drugs with good biological activity. The anti-proliferative activity of derivative **114** (Fig. 15, Table 15, IC_{50}: 0.022–0.056 μM) against A549, HeLa, PC-3, Bel-7402, Lovo, A2780, and MCF-7 cancer cell lines illustrated that *N*-methylation significantly enhanced the anti-proliferative activity. A mechanistic study illustrated that compound **114** inhibited tubulin polymerisation, disrupted microtubule organisation, and induced G2/M cell cycle arrest and apoptosis in A549 cells. Hence, compound **114** might potentially be a new tubulin-targeting agent that merits further study.[178]

The SAR revealed that the introduction of a heterocyclic ring at the C-6 position of indole was favourable for anti-proliferative activity, and derivative **115** (Fig. 15, Table 15, IC_{50}: 2–6 nM) showed excellent anti-proliferative activity against PC-3, A-549, THP-1, and MV4-11 cancer cell lines. Further study revealed that compound **115** arrested the cell cycle at the G2/M phase and fully inhibited tubulin polymerisation at 50 nM. Overall, compound **109** may potentially be used as a lead agent for the development of novel tubulin inhibitors.[179]

Derivative **116** (Fig. 15, Table 15, IC_{50}: 0.07 μM) was 3 fold more potent than combretastatin A-4 (CA-4) (IC_{50}: 0.21 μM) against HeLa cancer cells, and further study revealed that compound **116** greatly disrupted microtubule maturation in a concentration-dependent manner, induced G2/M cell cycle arrest, increased the ROS level and induced apoptosis in HeLa cells, which was associated with dissipation of mitochondrial membrane potential. Furthermore, compound **116** inhibited the migration of cancer cells, and in a HeLa xenograft mouse model, treatment with compound **116** significantly decreased tumour volume and inhibited tumour growth by 65.76% at a dose of 30 mg kg^{-1} without any weight

loss. Consequently, compound **116** can act as a novel tubulin inhibitor for cancer therapy.[180]

Derivative **117** (Fig. 15, Table 15, IC_{50}: 0.02–0.03 μM) was more potent than CA-4 (IC_{50}: 0.13 ≥ 10 μM) against HT-29 and A549 cancer lines, comparable to vinblastine (IC_{50}: 0.02–0.03 μM). Further experiments showed that compound **117** induced intracellular ROS generation and arrested HeLa cells in the G2/M phase by inducing apoptosis, which was associated with the loss of mitochondrial potential. Moreover, the compound exhibited high metabolic stability, with 48.6% remaining in human liver microsomes after 30 min, and possessed promising aqueous solubility with a solubility of 64.5 μM.[181]

Derivative **118** (Fig. 15, Table 15, IC_{50}: 37–62 nM) and derivative **119** (Fig. 15, Table 15, IC_{50}: 33–75 nM) inhibited the growth of MDA-MB-468, MDA-MB-23, and MDA-MB-436 cancer cell lines in a dose- and time-dependent manner. In addition, compounds **118** (IC_{50}: 0.1–0.3 nM) and **119** (IC_{50}: 16–62 nM) were generally more potent than vinblastine (IC_{50}: 53–766 nM) and paclitaxel (IC_{50}: 4900 to >10 000 nM) against PC-3, RD, and HeLa cancer cell lines, especially compound **118** at the micromolar level. Further studies showed that compounds **118** and **119** inhibited the Hh signalling pathway and tubulin polymerisation.[182]

Derivative **120** (Fig. 15, Table 15, IC_{50}: 0.08–5.89 μM) possessed excellent activity against HepG2, MCF-7, HeLa and A549 cancer cell lines, comparable to CA-4 (IC_{50}: 0.13–5.52 μM). SAR studies illustrated that the acylhydrazone group is essential for anti-proliferative activity. Mechanistic studies demonstrated that compound **120** induced significant ROS generation, mitochondrial depolarisation, G2/M cell cycle arrest, and apoptosis in A549 cancer cells. Western blot studies illustrated that compound **120** upregulated the levels of Bax, cleaved caspase-3 and PARP, and downregulated the levels of Bcl-2 and Bcl-xl. In the A549 xenografted mouse model, compound **120** strongly suppressed tumour growth by 70% at a dose of 30 mg kg^{-1}, and the weight showed no significant changes during the whole treatment period. Overall, compound **120** underwent further preclinical evaluation.[183]

Derivative **121** (Fig. 15, Table 15, IC_{50}: 0.015–0.053 μM) was more potent than CA-4 (IC_{50}: 0.031–0.058 μM) against the A549, HCT116, HeLa, and MCF-7 cancer cell lines. Further studies illustrated that compound **121** arrested the cell cycle in the G2/M phase, inhibited tubulin polymerisation, and bound to the colchicine-binding site of the tubulin polymer.[184]

Summary: curcumin and resveratrol-indole derivatives showed strong anti-tumor and anti-Alzheimer's disease activities. Among them, compound **108** had good antitumor activity against PC3, IC_{50}: 3.15–3.31 μM; derivative **111** showed 8–10 times higher inhibitory activity against Aβ and tau protein aggregation than curcumin, and derivative **115** showed nanomolar-level antitumor activity against PC-3, A-549, THP-1, and MV4-11. Therefore, compounds **108**, **111** and **115** are worthy of further study.

9. Quinone-indole derivatives

Quinones are relatively important active ingredients in natural products, which are natural products with an unsaturated cyclic diketone structure within the molecule or easily transformed into this quinone structure, including benzoquinone, naphthoquinone, and anthraquinone. Naphthoquinone is widely distributed in many kinds of higher plants, among which the high content includes

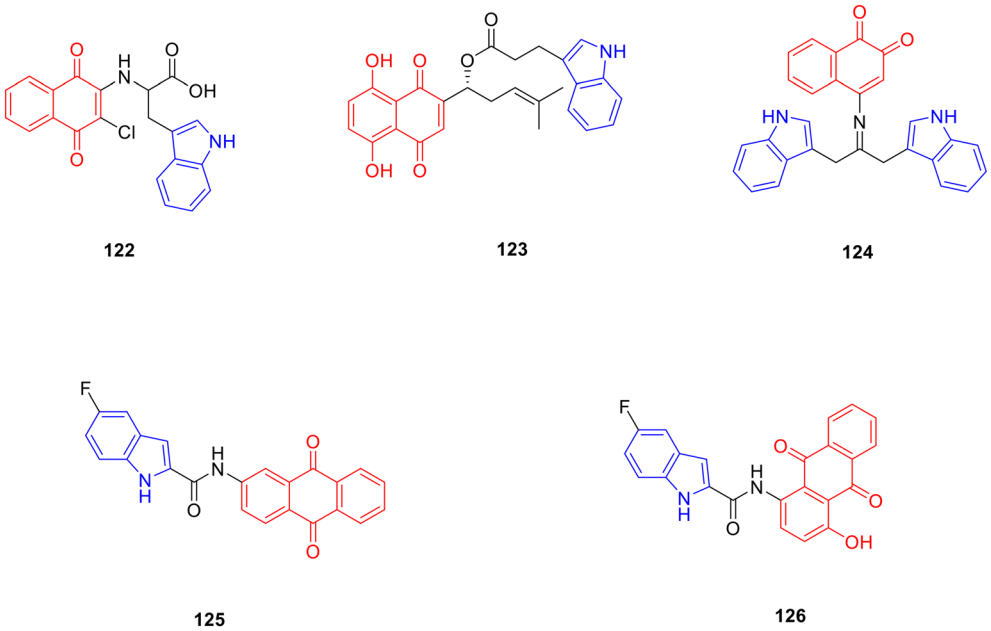

Fig. 16 Chemical structures of quinone-indole derivatives **122**–**126**.

Table 16 Biological activity of quinone-indole derivatives **122–124**

Compd.	Activity	Ref.
122	SiIHa cells: IC_{50} = 3.2 μM CaLo cells: IC_{50} = 2.69 μM C33-A cells: IC_{50} = 0.0034 μM	177
123	A578 cells: IC_{50} = 5 nM	178
Shikonin	A578 cells: IC_{50} = 0.46 μM	178
124	MCF-7 cells: IC_{50} = 11.33 μM HepG2 cells: IC_{50} = 10.14 μM MG-63 cells: IC_{50} = 13.85 μM	181
Naphthoquinone	MCF-7 cells: IC_{50} = 16.92 μM HepG2 cells: IC_{50} = 15.89 μM MG-63 cells: IC_{50} > 25 μM	181

Asteraceae, *Lamiaceae*, *Ebenaceae*, *etc.* Naphthoquinones are structurally divided into 1,4-naphthoquinone, 1,2-naphthoquinone, and 2,6-naphthoquinone.

1,4-Naphthoquinone is found in a variety of natural products and has various biological activities. It is considered a pharmacophore of bioactive compounds because of its various properties such as redox,[185] nucleophilic acceptance[186] and DNA intercalation.[187] Many 1,4-naphthoquinone derivatives have been synthesised and exhibit pharmacological activities, such as anti-tumor[188] and anti-viral activities.[189] Córdova-Rivas *et al.* designed and synthesized six 1,4-naphthoquinone derivatives with different substituents and determined their antitumor activities. Derivative **122** (Fig. 16, Table 16, IC_{50}: 0.0034–3.20 μM) exhibited promising activity against SiIHa, CaLo, and C33-A cancer cells. Further studies have shown that hydrophobic and aromatic amino acids have better inhibitory effects on cell proliferation.[190]

Shikonin is a natural product of 1,4-naphthoquinones, derived from the roots of *Lithospermum* species and has anti-tumor[191] and anti-viral activities.[192] Researchers designed and synthesized a series of shikonin derivatives, and evaluated the antitumor activity and antiviral activity of these derivatives. Derivative **123** (Fig. 16, Table 16, IC_{50}: 5 nM) was 92 fold more potent than shikonin (IC_{50}: 0.46 μM) against A578 cancer cells and induced G2/M cell cycle arrest.[193] Furthermore, shikonin-indole derivative **123** (IC_{50}: 0.011–0.052 μM) exhibited considerable activity against EV71, inhibited the expression levels of VP1 protein and phospho-p65 protein, and reduced the expression of mRNA in RD cells.[194]

1,2-Naphthoquinone, also known as β-naphthoquinone, is a nucleophilic receptor with anti-tumor and other pharmacological activities.[195] Shukla *et al.* designed and synthesized 18 1,2-naphthoquinone derivatives, expecting to obtain drugs with high anti-tumor activity. Derivative **124** (Fig. 16, Table 16, IC_{50}: 10.14–13.85 μM) exhibited comparable activity against MCF-7, HepG2 and MG-63 cancer cells, and was more potent than 1,2-naphthoquinone (IC_{50}: >15.89 μM). SAR analysis showed that the electron-absorbing substituents on the benzene ring contributed more to the anti-tumor activity than the electron-donating substituents.[196]

Anthraquinone derivatives are widely found in plants and have various pharmacological activities, including anti-dyslipidaemic effects.[197] Shattat *et al.* designed and synthesized seven different types of anthraquinone-indole derivatives, expecting to obtain hypolipidemic drugs with good biological activity. Because the whole molecule forms a conjugated system and C9 and C10 are at the highest oxygen level, natural anthraquinones are most commonly known as 9,10-anthraquinones. At a dose of 15 mg kg^{-1}, derivatives **125** (Fig. 16) and **126** (Fig. 16) significantly reduced plasma total cholesterol levels ($p < 0.0001$) and plasma triglyceride levels ($p < 0.0001$) and significantly increased HDL cholesterol levels after 12 and 24 h compared to hyperlipidaemic controls. Therefore, compounds **125** and **126** deserve further investigation as potential antihyperlipidaemic drugs.[198]

Summary: when the substituent on the benzene ring was an electron-withdrawing group, the activity was better. For example, compound **124** showed good activity against MCF-7, HepG2 and MG-63 cancer cells with IC_{50} values of 10.14–13.85 μM. Shikonin-indole derivative **123** had strong anti-tumor activity with an IC_{50} value of 5 nM, which was 92 fold that of shikonin. Therefore, compound **123** had further research value.

10. Conclusion

In this review, indole scaffolds have shown strong biological activities in anti-tumor, anti-inflammatory, anti-oxidation, anti-bacterial, hypolipidemic, anti-diabetic, anti-viral, anti-Alzheimer's disease, and anti-parasitic studies, among which anti-tumor is the most popular research field. Observing indole as a basic anti-tumor derivative, it can be found that most of the compounds with good biological activity have certain similarities with the connection sites, methods, properties and volume of substituents of indole. For example, podophyllotoxin and chalcone have the best anti-tumor activity when they are connected to the C5 position of indole. In addition, some indole derivatives with better pharmacological activity than lead compounds are also introduced in this paper. For example, compounds **103**, **104**, **118**, **119**, and **123** possessed high anti-proliferative activity against the tested cancer cells with IC_{50} values at nanomolar levels; compounds **83** and **90** showed broad-spectrum antifungal and antibacterial activities, respectively; and compounds **22**, **37**, **59**, **69**, **72**, **89**, **93**, **103** and **106** exhibited good *in vivo* efficacy; thus, these indole-modified natural product derivatives deserve further investigation. In summary, the indole structure will continue to be an important scaffold for the development of new highly bioactive drugs in future medicinal chemistry research, especially in the field of anti-tumor research. This review provides a comprehensive data resource of indole-natural product derivatives for researchers engaged in drug design and research, and helps medicinal chemistry researchers to design and develop new, efficient and low-toxic indole derivatives more rationally.

Conflicts of interest

The authors confirm that this research article has no conflict of interest.

Acknowledgements

This work was supported by the Higher Education Discipline Innovation Project (D18012), Key Projects of Jilin Province Science and Technology Development Plan (No. 20200404130YY), National Natural Science Foundation of China (No. 81960626, 82060628), Education Department Project of Jilin (No. JJKH20220559KJ), and Jilin Scientific and Technological Development Program (No. YDZJ202301ZYTS440). We would like to thank Editage (**https://www.editage.cn**) for English language editing.

References

1 A. Kumari and R. K. Singh, *Bioorg. Chem.*, 2020, **96**, 103578.
2 S. Dadashpour and S. Emami, *Eur. J. Med. Chem.*, 2018, **150**, 9–29.
3 S. Kumar, R. K. Singh, B. Patial, S. Goyal and T. R. Bhardwaj, *J. Enzyme Inhib. Med. Chem.*, 2016, **31**, 173–186.
4 X. Xiong, D. Zhang, J. Li, Y. Sun, S. Zhou, M. Yang, H. Shao and A. Li, *Chem. – Asian J.*, 2015, **10**, 869–872.
5 A. Chaudhuri, S. Haldar, H. Sun, R. E. Koeppe, 2nd and A. Chattopadhyay, *Biochim. Biophys. Acta*, 2014, **1838**, 419–428.
6 F. Wang, J. Bi, L. He, J. Chen, Q. Zhang, X. Hou and H. Xu, *Fitoterapia*, 2021, **153**, 104950.
7 M. Wang, B. Zhou, W. Cong, M. Zhang, Z. Li, Y. Li, S. Liang, K. Chen, D. Yang and Z. Wu, *Front. Pharmacol.*, 2021, **12**, 797605.
8 A. Dey, D. Roy, V. M. Mohture, M. Ghorai, M. H. Rahman, U. Anand, S. Dewanjee, R. Radha, M. Kumar, D. A. Prasanth, N. K. Jha, S. K. Jha, M. S. Shekhawat and D. K. Pandey, *Appl. Microbiol. Biotechnol.*, 2022, **106**, 4867–4883.
9 M. L. Zhou, J. R. Shao and Y. X. Tang, *Biotechnol. Appl. Biochem.*, 2009, **52**, 313–323.
10 A. Kumari and R. K. Singh, *Bioorg. Chem.*, 2019, **89**, 103021.
11 D. Xu and Z. Xu, *Curr. Top. Med. Chem.*, 2020, **20**, 1938–1949.
12 A. Dhiman, R. Sharma and R. K. Singh, *Acta Pharm. Sin. B*, 2022, **12**, 3006–3027.
13 Í. T. T. Jacob, F. O. S. Gomes, M. D. S. de Miranda, S. M. V. de Almeida, I. J. da Cruz-Filho, C. A. Peixoto, T. G. da Silva, D. R. M. Moreira, C. M. L. de Melo, J. F. de Oliveira and M. C. A. de Lima, *Pharmacol. Rep.*, 2021, **73**, 907–925.
14 A. Kumari and R. K. Singh, *Med. Chem.*, 2023, **19**, 163–173.
15 A. Kumari and R. K. Singh, *Chem. Biodiversity*, 2022, **19**, e202200290.
16 W. H. Chen, K. L. Li, X. P. Lin, S. R. Liao, B. Yang, X. F. Zhou, J. J. Wang, Y. H. Liu and J. F. Wang, *Nat. Prod. Res.*, 2021, **35**, 5266–5270.
17 A. Kumari and R. K. Singh, *Comb. Chem. High Throughput Screening*, 2023, **26**, 2077–2084.
18 K. H. Chang, C. H. Lin, H. C. Chen, H. Y. Huang, S. L. Chen, T. H. Lin, C. Ramesh, C. C. Huang, H. C. Fung, Y. R. Wu, H. J. Huang, G. J. Lee-Chen, H. M. Hsieh-Li and C. F. Yao, *CNS Neurosci. Ther.*, 2017, **23**, 45–56.
19 Y. Tamura, I. Morita, Y. Hinata, E. Kojima, H. Ozasa, H. Ikemoto, M. Asano, T. Wada, Y. Hayasaki-Kajiwara, T. Iwasaki and K. Matsumura, *Bioorg. Med. Chem. Lett.*, 2022, **68**, 128769.
20 A. Najmi, S. A. Javed, M. Al Bratty and H. A. Alhazmi, *Molecules*, 2022, **27**, 349.
21 B. Chopra and A. K. Dhingra, *Phytother. Res.*, 2021, **35**, 4660–4702.
22 S. S. Bommakanti, L. S. R. Kundeti, V. Saddanapu and K. Nagaiah, *ACS Omega*, 2020, **5**, 14069–14077.
23 H. Deng, X. Huang, C. Jin, C. M. Jin and Z. S. Quan, *Bioorg. Chem.*, 2020, **94**, 103467.
24 Q. K. Shen, H. Deng, S. B. Wang, Y. S. Tian and Z. S. Quan, *Eur. J. Med. Chem.*, 2019, **173**, 15–31.
25 T. L. Zhang, H. W. Yu and L. D. Ye, *ACS Synth. Biol.*, 2023, **12**, 639–656.
26 P. W. Huang, L. R. Wang, S. S. Geng, C. Ye, X. M. Sun and H. Huang, *Appl. Microbiol. Biotechnol.*, 2021, **105**, 4919–4930.
27 C. El-Baba, A. Baassiri, G. Kiriako, B. Dia, S. Fadlallah, S. Moodad and N. Darwiche, *Apoptosis.*, 2021, **26**, 491–511.
28 J. Grassmann, *Vitam. Horm.*, 2005, **72**, 505–535.
29 T. Yamaguchi, *Arch. Microbiol.*, 2022, **204**, 520.
30 V. N. Syrov, M. K. Abzalova, Z. A. Khushbaktova and M. B. Sultanov, *Pharm. Chem. J.*, 1985, **19**, 270–272.
31 M. K. Shanmugam, H. Shen, F. R. Tang, F. Arfuso, M. Rajesh, L. Wang, A. P. Kumar, J. Bian, B. C. Goh, A. Bishayee and G. Sethi, *Pharmacol. Res.*, 2018, **133**, 195–200.
32 J. Fang, T. Huang, M. Xia, L. Deng, X. Hao, Y. Wang and S. Mu, *Org. Biomol. Chem.*, 2018, **16**, 3026–3037.
33 T. An, H. Yin, Y. Lu and F. Liu, *Drug Des., Dev. Ther.*, 2022, **16**, 1255–1272.
34 S. Bommagani, J. Ponder, N. R. Penthala, V. Janganati, C. T. Jordan, M. J. Borrelli and P. A. Crooks, *Eur. J. Med. Chem.*, 2017, **136**, 393–405.
35 S. Slezakova and J. Ruda-Kucerova, *Anticancer Res.*, 2017, **37**, 5995–6003.
36 J. G. D'Angelo, C. Bordón, G. H. Posner, R. Yolken and L. Jones-Brando, *J. Antimicrob. Chemother.*, 2009, **63**, 146–150.
37 Y. Hu, N. Li, J. Zhang, Y. Wang, L. Chen and J. Sun, *Bioorg. Med. Chem. Lett.*, 2019, **29**, 1138–1142.
38 X. Ni, G. Hu and X. Cai, *Crit. Rev. Food Sci. Nutr.*, 2019, **59**, S71–S80.
39 A. S. Gurkan-Alp, M. Mumcuoglu, C. A. Andac, E. Dayanc, R. Cetin-Atalay and E. Buyukbingol, *Eur. J. Med. Chem.*, 2012, **58**, 346–354.
40 A. A. Farooqi, R. Attar, U. Y. Sabitaliyevich, N. Alaaeddine, D. P. de Sousa, B. Xu and W. C. Cho, *Cancers*, 2020, **12**, 2159.
41 S. Mehta, A. K. Sharma and R. K. Singh, *Mini-Rev. Med. Chem.*, 2021, **21**, 1556–1577.
42 Y. Song, Z. Xin, Y. Wan, J. Li, B. Ye and X. Xue, *Eur. J. Med. Chem.*, 2015, **90**, 695–706.

43 W. J. Kim, W. Kim, J. M. Bae, J. Gim and S. J. Kim, *Plants*, 2021, **10**, 1047.
44 H. Chen, C. Qiao, T. T. Miao, A. L. Li, W. Y. Wang and W. Gu, *J. Enzyme Inhib. Med. Chem.*, 2019, **34**, 1544–1561.
45 X. Liu, J. Xu, J. Zhou and Q. Shen, *Genes Dis.*, 2021, **8**, 448–462.
46 S. Thongnest, J. Boonsombat, H. Prawat, C. Mahidol and S. Ruchirawat, *Phytochemistry*, 2017, **134**, 98–105.
47 Y. Zhang, S. Yang, M. Zhang, Z. Wang, X. He, Y. Hou and G. Bai, *Nutrients*, 2019, **11**, 604.
48 L. De-la-Cruz-Martinez, C. Duran-Becerra, M. Gonzalez-Andrade, J. C. Paez-Franco, J. M. German-Acacio, J. Espinosa-Chavez, J. M. Torres-Valencia, J. Perez-Villanueva, J. F. Palacios-Espinosa, O. Soria-Arteche and F. Cortes-Benitez, *Molecules*, 2021, **26**, 4375.
49 H. Ding, X. Hu, X. Xu, G. Zhang and D. Gong, *Int. J. Biol. Macromol.*, 2018, **107**, 1844–1855.
50 N. K. Nema, N. Maity, B. Sarkar and P. K. Mukherjee, *Arch. Dermatol. Res.*, 2011, **303**, 247–252.
51 P. Wu, H. He, H. Ma, B. Tu, J. Li, S. Guo, S. Chen, N. Cao, W. Zheng, X. Tang, D. Li, X. Xu, X. Zheng, Z. Sheng, W. David Hong and K. Zhang, *Bioorg. Chem.*, 2021, **107**, 104580.
52 H. He, H. Li, T. Akanji, S. Niu, Z. Luo, D. Li, N. P. Seeram, P. Wu and H. Ma, *J. Enzyme Inhib. Med. Chem.*, 2021, **36**, 1665–1678.
53 V. Khwaza, O. O. Oyedeji and B. A. Aderibigbe, *Int. J. Mol. Sci.*, 2020, **21**, 5920.
54 A. L. Li, Y. Hao, W. Y. Wang, Q. S. Liu, Y. Sun and W. Gu, *Int. J. Mol. Sci.*, 2020, **21**, 2876.
55 W. Gu, Y. Hao, G. Zhang, S. F. Wang, T. T. Miao and K. P. Zhang, *Bioorg. Med. Chem. Lett.*, 2015, **25**, 554–557.
56 H. S. Pan, L. Li, H. B. Cui, L. N. Yang and Y. Q. Meng, *Acta Pharm. Sin.*, 2017, **52**, 1890–1894.
57 H. Fan, L. Geng, F. Yang, X. Dong, D. He and Y. Zhang, *Eur. J. Med. Chem.*, 2019, **176**, 61–67.
58 X. Liu, P. Zhao, X. Wang, L. Wang, Y. Zhu, Y. Song and W. Gao, *J. Exp. Clin. Cancer Res.*, 2019, **38**, 184.
59 K. Tang, J. Huang, J. Pan, X. Zhang and W. Lu, *RSC Adv.*, 2015, **5**, 19620–19623.
60 H. Lou, H. Li, S. Zhang, H. Lu and Q. Chen, *Molecules*, 2021, **26**, 5583.
61 Q. X. Huang, H. F. Chen, X. R. Luo, Y. X. Zhang, X. Yao and X. Zheng, *Curr. Med. Sci.*, 2018, **38**, 387–397.
62 E. F. Khusnutdinova, I. E. Smirnova, O. B. Kazakova, A. V. Petrova, N. T. T. Ha and D. Q. Viet, *Med. Chem. Res.*, 2017, **26**, 2737–2742.
63 E. F. Khusnutdinova, A. V. Petrova, H. N. T. Thu, A. L. T. Tu, T. N. Thanh, C. B. Thi, D. A. Babkov and O. B. Kazakova, *Bioorg. Chem.*, 2019, **88**, 102957.
64 Y. Zhao, C. H. Chen, S. L. Morris-Natschke and K. H. Lee, *Eur. J. Med. Chem.*, 2021, **215**, 113287.
65 K. Liu, X. Zhang, L. Xie, M. Deng, H. Chen, J. Song, J. Long, X. Li and J. Luo, *Pharmacol. Res.*, 2021, **164**, 105373.
66 P. Bhandari, N. K. Patel and K. K. Bhutani, *Bioorg. Med. Chem. Lett.*, 2014, **24**, 3596–3599.
67 M. A. Andrade, M. A. Braga, P. H. S. Cesar, M. V. C. Trento, M. A. Espósito, L. F. Silva and S. Marcussi, *Curr. Cancer Drug Targets*, 2018, **18**, 957–966.
68 L. Auezova, A. Najjar, M. Kfoury, S. Fourmentin and H. Greige-Gerges, *J. Appl. Microbiol.*, 2020, **128**, 710–720.
69 R. Yang, X. Chu, L. Sun, Z. Kang, M. Ji, Y. Yu, Y. Liu, Z. He and N. Gao, *Phytother. Res.*, 2018, **32**, 715–722.
70 F. Li, T. T. Yan, Y. Y. Fu, N. L. Zhang, L. Wang, Y. B. Zhang, J. Du and J. F. Liu, *Chem. Biodiversity*, 2021, **18**, e2001012.
71 Q. Guo and E. Jiang, *Curr. Top. Med. Chem.*, 2021, **21**, 1712–1724.
72 W. Zhao, L. He, T. L. Xiang and Y. J. Tang, *Eur. J. Med. Chem.*, 2019, **170**, 73–86.
73 H. W. Han, H. Y. Lin, D. L. He, Y. Ren, W. X. Sun, L. Liang, M. H. Du, D. C. Li, Y. C. Chu, M. K. Yang, X. M. Wang and Y. H. Yang, *Chem. Biodiversity*, 2018, **15**, e1800289.
74 M. Sathish, B. Kavitha, V. L. Nayak, Y. Tangella, A. Ajitha, S. Nekkanti, A. Alarifi, N. Shankaraiah, N. Nagesh and A. Kamal, *Eur. J. Med. Chem.*, 2018, **144**, 557–571.
75 L. Zhang, X. Zeng, X. Ren, N. Tao, C. Yang, Y. Xu, Y. Chen and J. Wang, *Med. Chem. Res.*, 2018, **28**, 81–94.
76 J. Wang, L. Long, Y. Chen, Y. Xu and L. Zhang, *Bioorg. Med. Chem. Lett.*, 2018, **28**, 1817–1824.
77 L. Zhang, F. Chen, J. Wang, Y. Chen, Z. Zhang, Y. Lin and X. Zhu, *RSC Adv.*, 2015, **5**, 97816–97823.
78 L. Zhang, L. Liu, C. Zheng, Y. Wang, X. Nie, D. Shi, Y. Chen, G. Wei and J. Wang, *Eur. J. Med. Chem.*, 2017, **131**, 81–91.
79 B. Cao, H. Chen, Y. Gao, C. Niu, Y. Zhang and L. Li, *Int. J. Mol. Med.*, 2015, **35**, 771–776.
80 T. Ai, S.-Y. Shi, L.-T. Chen, L. Li, B. Cao, Y. Gao, H. Chen and J. Zhou, *Chin. Chem. Lett.*, 2013, **24**, 37–40.
81 J. Liu, B. Cao, Y. Gao, M. Bai, X. Mei, H. Chen, Y. G. Jiang and D. J. Huang, *J. Asian Nat. Prod. Res.*, 2013, **15**, 985–992.
82 Z. H. Zhang, L. M. Zhang, G. Luo, S. Zhang, H. Chen and J. Zhou, *J. Asian Nat. Prod. Res.*, 2014, **16**, 527–534.
83 Y. E. Guo, H. Chen, S. Zuo, D. L. Liu, Y. L. Lu, J. J. Lv, S. P. Wen and T. C. Zhang, *J. Asian Nat. Prod. Res.*, 2011, **13**, 417–424.
84 N. Bhattarai, A. A. Kumbhar, Y. R. Pokharel and P. N. Yadav, *Mini-Rev. Med. Chem.*, 2021, **21**, 2996–3029.
85 R. Bhatia, A. Singh, B. Kumar and R. K. Rawal, *Key Heterocyclic Cores for Smart Anticancer Drug–Design Part II*, 2022, vol. 2, p. 35.
86 D. Feng, A. Zhang, Y. Yang and P. Yang, *Arch. Pharm.*, 2020, **353**, e1900380.
87 L. S. A. Carneiro, F. Almeida-Souza, Y. S. C. Lopes, R. C. V. Novas, K. B. A. Santos, C. B. P. Ligiero, K. D. S. Calabrese and C. D. Buarque, *Bioorg. Chem.*, 2021, **114**, 105141.
88 D. R. Vianna, G. Bubols, G. Meirelles, B. V. Silva, A. Da Rocha, M. Lanznaster, J. M. Monserrat, S. C. Garcia, G. Von Poser and V. L. Eifler-Lima, *Int. J. Mol. Sci.*, 2012, **13**, 7260–7270.
89 H. Li, Y. Yao and L. Li, *J. Pharm. Pharmacol.*, 2017, **69**, 1253–1264.

90 K. V. Sashidhara, A. Kumar, M. Kumar, R. Sonkar, G. Bhatia and A. K. Khanna, *Bioorg. Med. Chem. Lett.*, 2010, **20**, 4248–4251.

91 M. Y. Ali, S. Jannat, H. A. Jung, R. J. Choi, A. Roy and J. S. Choi, *Asian Pac. J. Trop. Med.*, 2016, **9**, 103–111.

92 P. R. Kamath, D. Sunil, A. A. Ajees, K. S. Pai and S. Das, *Bioorg. Chem.*, 2015, **63**, 101–109.

93 P. R. Kamath, D. Sunil, M. M. Joseph, A. A. Abdul Salam and T. T. Sreelekha, *Eur. J. Med. Chem.*, 2017, **136**, 442–451.

94 R. Pathoor and D. Bahulayan, *New J. Chem.*, 2018, **42**, 6810–6816.

95 O. Galayev, Y. Garazd, M. Garazd and R. Lesyk, *Eur. J. Med. Chem.*, 2015, **105**, 171–181.

96 X. C. Yang, P. L. Zhang, K. V. Kumar, S. Li, R. X. Geng and C. H. Zhou, *Eur. J. Med. Chem.*, 2022, **232**, 114192.

97 A. S. Rathod, S. S. Godipurge and J. S. Biradar, *Int. J. Pharm. Pharm. Sci.*, 2017, **9**, 233–240.

98 J. N. Sangshetti, F. A. Kalam Khan, A. A. Kulkarni, R. H. Patil, A. M. Pachpinde, K. S. Lohar and D. B. Shinde, *Bioorg. Med. Chem. Lett.*, 2016, **26**, 829–835.

99 M. Mollazadeh, M. Mohammadi-Khanaposhtani, Y. Valizadeh, A. Zonouzi, M. A. Faramarzi, M. Kiani, M. Biglar, B. Larijani, H. Hamedifar, M. Mahdavi and M. H. Hajimiri, *Med. Chem.*, 2021, **17**, 264–272.

100 K. V. Sashidhara, K. B. Rao, R. Sonkar, R. K. Modukuri, Y. S. Chhonker, P. Kushwaha, H. Chandasana, A. K. Khanna, R. S. Bhatta, G. Bhatia, M. K. Suthar, J. K. Saxena, V. Kumar and M. I. Siddiqi, *MedChemComm*, 2016, **7**, 1858–1869.

101 S. Ghanei-Nasab, M. Khoobi, F. Hadizadeh, A. Marjani, A. Moradi, H. Nadri, S. Emami, A. Foroumadi and A. Shafiee, *Eur. J. Med. Chem.*, 2016, **121**, 40–46.

102 Y. Zou, N. Lu, X. Yang, Z. Xie, X. Lei, X. Liu, Y. Li, S. Huang, G. Tang and Z. Wang, *RSC Med. Chem.*, 2023, **14**, 1172–1185.

103 X. Zhang, D. Lin, R. Jiang, H. Li, J. Wan and H. Li, *Oncol. Rep.*, 2016, **36**, 271–278.

104 K. Zduńska, A. Dana, A. Kolodziejczak and H. Rotsztejn, *Skin Pharmacol. Physiol.*, 2018, **31**, 332–336.

105 Q. Yu and L. Fan, *Food Chem.*, 2021, **352**, 129369.

106 B. Zolfaghari, Z. Yazdiniapour, M. Sadeghi, M. Akbari, R. Troiano and V. Lanzotti, *Phytochem. Anal.*, 2021, **32**, 84–90.

107 J. Zang, B. Shi, X. Liang, Q. Gao, W. Xu and Y. Zhang, *Bioorg. Med. Chem.*, 2017, **25**, 2666–2675.

108 M. Benchekroun, L. Ismaili, M. Pudlo, V. Luzet, T. Gharbi, B. Refouvelet and J. Marco-Contelles, *Future Med. Chem.*, 2015, **7**, 15–21.

109 I. Pachón-Angona, H. Martin, S. Chhor, M. J. Oset-Gasque, B. Refouvelet, J. Marco-Contelles and L. Ismaili, *Future Med. Chem.*, 2019, **11**, 3097–3108.

110 K. Takao, K. Toda, T. Saito and Y. Sugita, *Chem. Pharm. Bull.*, 2017, **65**, 1020–1027.

111 N. C. Desai, H. C. Somani, H. K. Mehta, D. J. Jadeja, A. G. Khasiya and V. M. Khedkar, *SAR QSAR Environ. Res.*, 2022, **33**, 89–109.

112 A. Elkamhawy, N. K. Oh, N. A. Gouda, M. H. Abdellattif, S. O. Alshammari, M. A. S. Abourehab, Q. A. Alshammari, A. Belal, M. Kim, A. A. Al-Karmalawy and K. Lee, *Metabolites*, 2023, **13**, 141.

113 S. Qiao, C. Lv, Y. Tao, Y. Miao, Y. Zhu, W. Zhang, D. Sun, X. Yun, Y. Xia, Z. Wei and Y. Dai, *Cancer Lett.*, 2020, **491**, 162–179.

114 Y. N. Lu, X. D. Zhao, X. Xu, J. Piao, F. Aosai, Y. B. Li, L. X. Shen, S. Y. Shi, G. H. Xu, J. Ma, H. N. Piao, X. Jin and L. X. Piao, *Int. Immunopharmacol.*, 2020, **84**, 106539.

115 Q. Chen, L. Yang, M. Han, E. Cai and Y. Zhao, *Biomed. Pharmacother.*, 2016, **84**, 1792–1801.

116 H. B. Zhang, Q. K. Shen, H. Wang, C. Jin, C. M. Jin and Z. S. Quan, *Eur. J. Med. Chem.*, 2018, **158**, 414–427.

117 L. G. S. Ponte, I. C. B. Pavan, M. C. S. Mancini, L. G. S. da Silva, A. P. Morelli, M. B. Severino, R. M. N. Bezerra and F. M. Simabuco, *Molecules*, 2021, **26**, 2029.

118 S. J. Maleki, J. F. Crespo and B. Cabanillas, *Food Chem.*, 2019, **299**, 125124.

119 F. Farhadi, B. Khameneh, M. Iranshahi and M. Iranshahy, *Phytother. Res.*, 2019, **33**, 13–40.

120 J. Xiao, M. Gao, Q. Diao and F. Gao, *Curr. Top. Med. Chem.*, 2021, **21**, 348–362.

121 M. Xu, P. Wu, F. Shen, J. Ji and K. P. Rakesh, *Bioorg. Chem.*, 2019, **91**, 103133.

122 G. Wang, C. Li, L. He, K. Lei, F. Wang, Y. Pu, Z. Yang, D. Cao, L. Ma, J. Chen, Y. Sang, X. Liang, M. Xiang, A. Peng, Y. Wei and L. Chen, *Bioorg. Med. Chem.*, 2014, **22**, 2060–2079.

123 D. Preti, R. Romagnoli, R. Rondanin, B. Cacciari, E. Hamel, J. Balzarini, S. Liekens, D. Schols, F. Estevez-Sarmiento, J. Quintana and F. Estevez, *J. Enzyme Inhib. Med. Chem.*, 2018, **33**, 1225–1238.

124 S. Zhang, B. An, J. Li, J. Hu, L. Huang, X. Li and A. S. C. Chan, *Org. Biomol. Chem.*, 2017, **15**, 7404–7410.

125 H. Mirzaei, M. Shokrzadeh, M. Modanloo, A. Ziar, G. H. Riazi and S. Emami, *Bioorg. Chem.*, 2017, **75**, 86–98.

126 H. Mirzaei, M. Abastabar and S. Emami, *Comput. Biol. Chem.*, 2020, **84**, 107189.

127 B. Du, X. Liu, X. Luan, W. Zhang and C. Zhuang, *Bioorg. Chem.*, 2023, **135**, 106531.

128 A. Rauf, R. Khan, M. Raza, H. Khan, S. Pervez, V. De Feo, F. Maione and N. Mascolo, *Fitoterapia*, 2015, **103**, 129–135.

129 P. Singh, J. Kaur, G. Singh and R. Bhatti, *J. Med. Chem.*, 2015, **58**, 5989–6001.

130 P. Singh, S. Shaveta, S. Sharma and R. Bhatti, *Bioorg. Med. Chem. Lett.*, 2014, **24**, 77–82.

131 Y. B. Ji, W. J. Chen, T. Z. Shan, B. Y. Sun, P. C. Yan and W. Jiang, *Chem. Biodiversity*, 2020, **17**, e1900640.

132 N. T. Nhan, P. H. Nguyen, M. H. Tran, P. D. Nguyen, D. T. Tran and D. C. To, *J. Asian Nat. Prod. Res.*, 2021, **23**, 414–422.

133 X. Chen, J. Leng, K. P. Rakesh, N. Darshini, T. Shubhavathi, H. K. Vivek, N. Mallesha and H. L. Qin, *MedChemComm*, 2017, **8**, 1706–1719.

134 R. Haudecoeur, A. Ahmed-Belkacem, W. Yi, A. Fortuné, R. Brillet, C. Belle, E. Nicolle, C. Pallier, J. M. Pawlotsky and A. Boumendjel, *J. Med. Chem.*, 2011, **54**, 5395–5402.

135 A. Meguellati, A. Ahmed-Belkacem, W. Yi, R. Haudecoeur, M. Crouillere, R. Brillet, J. M. Pawlotsky, A. Boumendjel and M. Peuchmaur, *Eur. J. Med. Chem.*, 2014, **80**, 579–592.

136 N. Xie, F. P. Gomes, V. Deora, K. Gregory, T. Vithanage, Z. D. Nassar, P. J. Cabot, D. Sturgess, P. N. Shaw and M. O. Parat, *Brain, Behav., Immun.*, 2017, **61**, 244–258.

137 S. Obeng, H. Wang, A. Jali, D. L. Stevens, H. I. Akbarali, W. L. Dewey, D. E. Selley and Y. Zhang, *ACS Chem. Neurosci.*, 2019, **10**, 1075–1090.

138 C. Liu, S. Yang, K. Wang, X. Bao, Y. Liu, S. Zhou, H. Liu, Y. Qiu, T. Wang and H. Yu, *Biomed. Pharmacother.*, 2019, **120**, 109543.

139 H. Ur Rashid, S. Rasool, Y. Ali, K. Khan and M. A. U. Martines, *Bioorg. Chem.*, 2020, **99**, 103863.

140 Y. Xu, L. Wu, H. U. Rashid, D. Jing, X. Liang, H. Wang, X. Liu, J. Jiang, L. Wang and P. Xie, *Eur. J. Med. Chem.*, 2018, **156**, 479–492.

141 Z. Li, M. Luo, B. Cai, R. Haroon Ur, M. Huang, J. Jiang, L. Wang and L. Wu, *Eur. J. Med. Chem.*, 2018, **157**, 665–682.

142 G. Hu, C. Cao, Z. Deng, J. Li, X. Zhou, Z. Huang and C. Cen, *Oncol. Lett.*, 2021, **21**, 66.

143 Z. Li, M. Luo, B. Cai, L. Wu, M. Huang, R. Haroon Ur, J. Jiang and L. Wang, *Bioorg. Med. Chem. Lett.*, 2018, **28**, 677–683.

144 L. Li, J. Li, L. Ma, H. Shang and Z. Zou, *Bioorg. Chem.*, 2023, **134**, 106341.

145 L. M. Ortiz, P. Lombardi, M. Tillhon and A. I. Scovassi, *Molecules*, 2014, **19**, 12349–12367.

146 B. Mistry, Y.-S. Keum and D. H. Kim, *Res. Chem. Intermed.*, 2015, **42**, 3241–3256.

147 H. W. Liu, Q. T. Ji, G. G. Ren, F. Wang, F. Su, P. Y. Wang, X. Zhou, Z. B. Wu, Z. Li and S. Yang, *J. Agric. Food Chem.*, 2020, **68**, 12558–12568.

148 J. Dai, W. Dan, N. Li and J. Wang, *Eur. J. Med. Chem.*, 2018, **157**, 333–338.

149 A. V. Zolottsev, A. S. Latysheva, V. S. Pokrovsky, I. I. Khan and A. Y. Misharin, *Eur. J. Med. Chem.*, 2021, **210**, 113089.

150 G. X. Yang, Y. Huang, L. L. Zheng, L. Zhang, L. Su, Y. H. Wu, J. Li, L. C. Zhou, J. Huang, Y. Tang, R. Wang and L. Ma, *Eur. J. Med. Chem.*, 2020, **187**, 111913.

151 H. Zhang, J. Xu, M. Wang, X. Xia, R. Dai and Y. Zhao, *Steroids*, 2020, **161**, 108690.

152 P. Kovács, T. Csonka, T. Kovács, Z. Sári, G. Ujlaki, A. Sipos, Z. Karányi, D. Szeőcs, C. Hegedűs, K. Uray, L. Jankó, M. Kiss, B. Kiss, D. Laoui, L. Virág, G. Méhes, P. Bai and E. Mikó, *Cancers*, 2019, **11**, 1522.

153 M. Incerti, S. Russo, D. Callegari, D. Pala, C. Giorgio, I. Zanotti, E. Barocelli, P. Vicini, F. Vacondio, S. Rivara, R. Castelli, M. Tognolini and A. Lodola, *J. Med. Chem.*, 2017, **60**, 787–796.

154 X. L. He, Y. Xing, X. Z. Gu, J. X. Xiao, Y. Y. Wang, Z. Yi and W. W. Qiu, *Steroids*, 2017, **125**, 54–60.

155 W. Tan, M. Pan, H. Liu, H. Tian, Q. Ye and H. Liu, *OncoTargets Ther.*, 2017, **10**, 3467–3474.

156 L. Hu, M. Bu, T. Cao, H. Li, M. Guo, Y. Zhou, N. Zhang, C. Zeng and Y. Wang, *Heterocycles*, 2017, **94**, 691–701.

157 H. Li, H. Wang, J. Wang, Y. Lin, Y. Ma and M. Bu, *Steroids*, 2020, **153**, 108471.

158 L. Chen, W. Mai, M. Chen, J. Hu, Z. Zhuo, X. Lei, L. Deng, J. Liu, N. Yao, M. Huang, Y. Peng, W. Ye and D. Zhang, *Pharmacol. Res.*, 2017, **123**, 130–142.

159 L. J. Deng, L. H. Wang, C. K. Peng, Y. B. Li, M. H. Huang, M. F. Chen, X. P. Lei, M. Qi, Y. Cen, W. C. Ye, D. M. Zhang and W. M. Chen, *J. Med. Chem.*, 2017, **60**, 5320–5333.

160 E. Pietri, I. Massa, S. Bravaccini, S. Ravaioli, M. M. Tumedei, E. Petracci, C. Donati, A. Schirone, F. Piacentini, L. Gianni, M. Nicolini, E. Campadelli, A. Gennari, A. Saba, B. Campi, L. Valmorri, D. Andreis, F. Fabbri, D. Amadori and A. Rocca, *Oncologist*, 2019, **24**, e197–e205.

161 J. Cui, L. Liu, D. Zhao, C. Gan, X. Huang, Q. Xiao, B. Qi, L. Yang and Y. Huang, *Steroids*, 2015, **95**, 32–38.

162 N. Mahmoudi, Z. Kiasalari, T. Rahmani, A. Sanaierad, S. Afshin-Majd, G. Naderi, T. Baluchnejadmojarad and M. Roghani, *Neuropsychobiology*, 2021, **80**, 25–35.

163 L. C. Zhou, Y. F. Liang, Y. Huang, G. X. Yang, L. L. Zheng, J. M. Sun, Y. Li, F. L. Zhu, H. W. Qian, R. Wang and L. Ma, *Eur. J. Med. Chem.*, 2021, **219**, 113426.

164 I. E. Smirnova, O. B. Kazakova, D. Q. Viet, N. T. Thuc, P. T. Linh and D. T. T. Huong, *Med. Chem. Res.*, 2014, **24**, 2177–2182.

165 D. Vervandier-Fasseur and N. Latruffe, *Molecules*, 2019, **24**, 4506.

166 J. Gan, X. Zhang, C. Ma, L. Sun, Y. Feng, Z. He and H. Zhang, *J. Food Sci.*, 2022, **87**, 1244–1256.

167 G. C. Luque, M. Moya, M. L. Picchio, V. Bagnarello, I. Valerio, J. Bolaños, M. Vethencourt, S. H. Gamboa, L. C. Tomé, R. J. Minari and D. Mecerreyes, *Polymers*, 2023, **15**, 1076.

168 A. Giordano and G. Tommonaro, *Nutrients*, 2019, **11**, 2376.

169 M. Tang and C. Taghibiglou, *J. Alzheimer's Dis.*, 2017, **58**, 1003–1016.

170 M. Nayakula, M. K. Jeengar, V. G. M. Naidu and N. Chella, *Eur. J. Drug Metab. Pharmacokinet.*, 2023, **48**, 189–199.

171 P. V. Sri Ramya, S. Angapelly, L. Guntuku, C. Singh Digwal, B. Nagendra Babu, V. G. M. Naidu and A. Kamal, *Eur. J. Med. Chem.*, 2017, **127**, 100–114.

172 A. Theppawong, T. Van de Walle, C. Grootaert, M. Bultinck, T. Desmet, J. Van Camp and M. D'Hooghe, *ChemistryOpen*, 2018, **7**, 381–392.

173 T. Van de Walle, A. Theppawong, C. Grootaert, S. De Jonghe, L. Persoons, D. Daelemans, K. Van Hecke, J. Van Camp and M. D'hooghe, *Monatsh. Chem.*, 2019, **150**, 2045–2051.

174 M. Okuda, I. Hijikuro, Y. Fujita, T. Teruya, H. Kawakami, T. Takahashi and H. Sugimoto, *Bioorg. Med. Chem. Lett.*, 2016, **26**, 5024–5028.

175 R. Rajagopalan, S. Subramanian, S. Pajaniradje, R. Tumdam, M. Hoda and A. Dasgupta, *J. Cancer Res. Ther.*, 2023, **19**, 265–272.

176 Z. Zheng, X. Li, P. Chen, Y. Zou, X. Shi, X. Li, E. Young Kim, J. Liao, J. Yang, N. Chattipakorn, G. Wu, Q. Tang, W.-J. Cho and G. Liang, *Bioorg. Chem.*, 2023, **136**, 106557.
177 A. Rauf, M. Imran, M. S. Butt, M. Nadeem, D. G. Peters and M. S. Mubarak, *Crit. Rev. Food Sci. Nutr.*, 2018, **58**, 1428–1447.
178 J. Yan, J. Hu, B. An, L. Huang and X. Li, *Eur. J. Med. Chem.*, 2017, **125**, 663–675.
179 G. La Regina, R. Bai, A. Coluccia, V. Naccarato, V. Famiglini, M. Nalli, D. Masci, A. Verrico, P. Rovella, C. Mazzoccoli, E. Da Pozzo, C. Cavallini, C. Martini, S. Vultaggio, G. Dondio, M. Varasi, C. Mercurio, E. Hamel, P. Lavia and R. Silvestri, *Eur. J. Med. Chem.*, 2018, **152**, 283–297.
180 S. Hua, F. Chen, X. Wang and S. Gou, *Eur. J. Med. Chem.*, 2020, **189**, 112041.
181 G. La Regina, R. Bai, W. M. Rensen, E. Di Cesare, A. Coluccia, F. Piscitelli, V. Famiglini, A. Reggio, M. Nalli, S. Pelliccia, E. Da Pozzo, B. Costa, I. Granata, A. Porta, B. Maresca, A. Soriani, M. L. Iannitto, A. Santoni, J. Li, M. Miranda Cona, F. Chen, Y. Ni, A. Brancale, G. Dondio, S. Vultaggio, M. Varasi, C. Mercurio, C. Martini, E. Hamel, P. Lavia, E. Novellino and R. Silvestri, *J. Med. Chem.*, 2013, **56**, 123–149.
182 G. La Regina, R. Bai, A. Coluccia, V. Famiglini, S. Pelliccia, S. Passacantilli, C. Mazzoccoli, V. Ruggieri, A. Verrico, A. Miele, L. Monti, M. Nalli, R. Alfonsi, L. Di Marcotullio, A. Gulino, B. Ricci, A. Soriani, A. Santoni, M. Caraglia, S. Porto, E. Da Pozzo, C. Martini, A. Brancale, L. Marinelli, E. Novellino, S. Vultaggio, M. Varasi, C. Mercurio, C. Bigogno, G. Dondio, E. Hamel, P. Lavia and R. Silvestri, *J. Med. Chem.*, 2015, **58**, 5789–5807.
183 Y. T. Duan, R. J. Man, D. J. Tang, Y. F. Yao, X. X. Tao, C. Yu, X. Y. Liang, J. A. Makawana, M. J. Zou, Z. C. Wang and H. L. Zhu, *Sci. Rep.*, 2016, **6**, 25387.
184 A. Kamal, G. B. Kumar, S. Polepalli, A. B. Shaik, V. S. Reddy, M. K. Reddy, R. Reddy Ch, R. Mahesh, J. S. Kapure and N. Jain, *ChemMedChem*, 2014, **9**, 2565–2579.
185 C. C. Shen, S. N. Afraj, C. C. Hung, B. D. Barve, L. Y. Kuo, Z. H. Lin, H. O. Ho and Y. H. Kuo, *Bioorg. Med. Chem. Lett.*, 2021, **41**, 127976.
186 C. Ibis, A. F. Tuyun, H. Bahar, S. S. Ayla, M. V. Stasevych, R. Y. Musyanovych, O. Komarovska-Porokhnyavets and V. Novikov, *Med. Chem. Res.*, 2014, **23**, 2140–2149.
187 M. S. Farias, C. T. Pich, M. R. Kviecinski, N. C. Bucker, K. B. Felipe, F. O. Da Silva, T. M. Günther, J. F. Correia, D. Ríos, J. Benites, J. A. Valderrama, P. B. Calderon and R. C. Pedrosa, *Mol. Med. Rep.*, 2014, **10**, 405–410.
188 J. Palacios, J. Benites, G. I. Owen, P. Morales, M. Chiong, C. R. Nwokocha, A. Paredes and F. Cifuentes, *J. Cardiovasc. Pharmacol.*, 2021, **77**, 245–252.
189 V. K. Tandon, R. V. Singh and D. B. Yadav, *Bioorg. Med. Chem. Lett.*, 2004, **14**, 2901–2904.
190 S. Cordova-Rivas, J. G. Araujo-Huitrado, E. Rivera-Avalos, I. L. Escalante-Garcia, S. M. Duron-Torres, Y. Lopez-Hernandez, H. Hernandez-Lopez, L. Lopez, D. de Loera and J. A. Lopez, *Molecules*, 2020, **25**, 2058.
191 J. C. Boulos, M. Rahama, M. F. Hegazy and T. Efferth, *Cancer Lett.*, 2019, **459**, 248–267.
192 Y. Zhang, H. Han, H. Qiu, H. Lin, L. Yu, W. Zhu, J. Qi, R. Yang, Y. Pang, X. Wang, G. Lu and Y. Yang, *Biomed. Pharmacother.*, 2017, **93**, 636–645.
193 X. M. Wang, H. Y. Lin, W. Y. Kong, J. Guo, J. Shi, S. C. Huang, J. L. Qi, R. W. Yang, H. W. Gu and Y. H. Yang, *Chem. Biol. Drug Des.*, 2014, **83**, 334–343.
194 Y. Zhang, H. Han, L. Sun, H. Qiu, H. Lin, L. Yu, W. Zhu, J. Qi, R. Yang, Y. Pang, X. Wang, G. Lu and Y. Yang, *Braz. J. Med. Biol. Res.*, 2017, **50**, e6586–e6594.
195 R. Nakagawa, H. Tateishi, M. O. Radwan, T. Chinen, H. Ciftci, K. Iwamaru, N. Baba, Y. Tominaga, R. Koga, T. Toma, J. I. Inoue, K. Umezawa, M. Fujita and M. Otsuka, *Chem. Pharm. Bull.*, 2022, **70**, 477–482.
196 S. Shukla, R. S. Srivastava, S. K. Shrivastava, A. Sodhi and P. Kumar, *Med. Chem. Res.*, 2012, **22**, 1604–1617.
197 S. K. Mishra, S. Tiwari, A. Shrivastava, S. Srivastava, G. K. Boudh, S. K. Chourasia, U. Chaturvedi, S. S. Mir, A. K. Saxena, G. Bhatia and V. Lakshmi, *J. Nat. Med.*, 2014, **68**, 363–371.
198 G. Shattat, T. Al-Qirim, G. A. Sheikha, Y. Al-Hiari, K. Sweidan, R. Al-Qirim, S. Hikmat, L. Hamadneh and S. Al-Kouz, *J. Enzyme Inhib. Med. Chem.*, 2013, **28**, 863–869.